Immobilisation of Metal in Quartz Sands by Ball Milling

Zhang, ZhengXi

A thesis submitted to

Auckland University of Technology

in fulfilment of the requirements for the degree of

Master of Philosophy (MPhil)

2008

Faculty of Health and Environmental Science

Primary Supervisor: Dr. John Robertson

Acknowledgment

I especially thank Dr. John Robertson for his guide, support, and reviewing this thesis.

Thanks to Dr. Roger Whiting, Mr. Mark Duxbury and Dr. Richard Anstiss for their valuable advice and help during the project. Thanks to Dr. Neil Binnie for his help with statistical analysis.

Thanks to Mr. Chris Whyburd, Mrs. Wang Yan, and Mr. Percy Perera, for help with preparing laboratory equipment and Mr. Tim Yong for the help in quartz particle size measurement.

Thanks to Mr. Sha DeReng for his valuable suggestions in quartz hydrofluoric acid digestion.

My deepest gratitude is to my family for much love, encouragement, and support during the course of this study.

Abstract

Previous work has shown that when inorganic compounds are milled with quartz in a high energy ball mill the elements are sequestered into the quartz matrix and cannot be easily recovered by simple extraction methods. In this study lead (II) oxide, copper (II) oxide, magnesium oxide, zinc oxide and sodium hydroxide were milled with quartz sand and the recoveries of the metals investigated in detail. The standard EPA3050B method (acid digestion of sediments, sludge and soils) for extractable metals was compared to exhaustive HF digestion method based on ASTM C146-94a (test methods for chemical analysis of glass sand) and UDC 666.123:543.06 (chemical analysis of soda-lime and borosilicate glass). From these two analyses the total recovery of metals was determined.

It was found that the elements extracted by the EPA3050B method decreased in an approximately logarithmic way with milling time. The metals are apparently strongly sequestered into the fractured quartz. Total HF digestion of the insoluble matrix gave good recovery of the "lost" elements. A reliable analytical procedure has been developed and the mechanisms leading to this sequestering are discussed.

Particle size analysis and electron microscopy of milled samples support a process of brittle alloy formation as the proposed mechanism whereby the elements are sequestered into the milled quartz.

Table of contents

List of figures

List of tables

Statement of originality

"I hereby declare that this submission is my own work and that, to the best of my knowledge and belief, it contains no material previously published or written by another person nor material which to a substantial extent has been accepted for the qualification of any other degree or diploma of a university or other institution of higher learning, except where due acknowledgment is made in the Acknowledgments"

Signed _____

Date _____

Abbreviations

AA	Atomic absorption
ASTM	American society for testing and materials
BPR	Balls to powder ratio
Conc.	Concentration
CR	Charge ratio
DDD	Dichlorodiphenyl dichloroethane
DDE	Dichlorodiphenyl dichloroethene
DDT	Dichlorodiphenyl Trichloroethane
EDS	Energy dispersive spectroscopy
EPA	Environmental protection agency
EPA3050B	Acid digestion of sediments sludge and soils (United States of America Environmental protection agency 3050B digestion method)
HF test	Hydrofluoric acid test (digestion)
ICP	Inductively coupled plasma
MA	Mechanical alloying
MD	Mechanical disordering and destruction
MG	Mechanical grinding
MM	Mechanical milling
MS	Mechanochemical synthesis
PAH	Poly aromatic hydrocarbon
RM	Reactive milling or Reaction milling
SEM	Scanning electron microscope
UDC	Universal decimal classification
XRD	X-ray diffraction
XRF	X-ray fluorescence

Chapter 1. Introduction

Background

High energy ball milling is rapidly developing a place as a potentially effective and inexpensive way of treating polluted soil. Earlier work by Bellingham (2006) where DDT and some other chlorinated pesticides were subjected to intense ball milling in a quartz sand matrix showed that the method was highly effective for destroying organic compounds. However, when attempts were made to balance the chlorine, significant amounts of chlorine from the pesticides were apparently "lost" and could not be accounted for even after exhaustive extraction of the remaining milled material with water. The mills were considered sealed systems and there was no evidence that any chlorine was lost as volatile material. It was assumed that the chlorine was as chloride and should have been very soluble in water.

Subsequent milling experiments with (inorganic) sodium chloride and quartz (Mok, 2006) confirmed that， although as much as 80% of the chloride could not be recovered from the resulting mixture by water extraction， x-ray fluorescence (XRF) analysis of these samples showed there was no loss of total chlorine. This confirmed that even in a simple experiment like this, some of the chlorine (presumably as chloride) had been sequestered in some way into the quartz. Further brief experiments (personal communication John Robertson) with magnesium oxide and quartz suggested that 40% – 50% of the magnesium was trapped in some way in the quartz after a few hours of milling.

The inability to account for all the elements when destroying hazardous pesticides creates an obvious doubt about the validity of the method but this and the magnesium experiments also suggest the possibility that elements such as heavy metals could also be effectively trapped into suitable mineral matrices and thus safely immobilised in the environment. Because the mechanism was quite uncertain the expression "sequestered" was adopted.

Thus there was a need to investigate the mechanisms causing elements to be sequestered and importantly， at the same time, develop a robust analytical procedure to provide a reliable quantitative recovery of soluble and sequestered elements from milled mixtures.

1.1 Definition and history of mechanochemical process and Mechanochemistry

1.1.1 Definition of mechanochemistry

Mechanochemistry is a branch of chemistry dealing with the composition of substances and their properties where the reaction is induced by mechanical energy. Sohma (1989) defined it as: "a branch of chemistry in which chemical phenomena, such as chemical reactions and changes in crystalline structures, induced by mechanical actions like fracture and large deformations, are studied." (p.453) This can be simplified as: during the milling of solids, chemical reactions occur (Fernández-Bertran, 1999).

1.1.2 History of mechanochemistry

At the beginning of the 20^{th} century, Nernst classified chemistry into several different fields according to the type of energy facilitating the reaction e.g. thermo chemistry, electrochemistry, photochemistry etc. (Gilman, 1996). Boldyrev (1995) noted that as early as 1919, Ostwald had already realized the importance of identifying a special branch of chemistry in which mechanical energy alone initiated the chemical process.

Recently some researchers noted that the first recorded mechanochemical phenomenon was preparing mercury from cinnabar in "De Lapidibus" or "On Stones" by Theophrastus of Ephesus (371-286 B.C.) Theophrastus was a student of Aristotle. (Boldyrev & Tkácová, 2000). Beyer and Clausen-Schaumann (2005) thought the reaction was probably:

$$HgS + Cu \rightarrow Hg + CuS \qquad \text{Equation 1.1}$$

But it is more commonly accepted that Lea (Heinicke, 1984; Fernández-Bertran, 1999) was the first person in the 19th century to notice the difference between mechanochemical and thermochemical processing. Mechanochemical processing will decompose silver and mercury halides to give the metals and chlorine during attrition in a mortar (equation 1.2) (Fernández-Bertran, 1999) but when heated, mercury chloride will sublime and silver halides will melt undecomposed as a result (equation 1.3 and equation 1.4). "The local heating was not considered to be the cause of the initiation of the decomposition reaction." (Boldyrev & Tkácová, 2000, p.121).

$HgCl_2 + 2AgCl \rightarrow Hg + 2Ag + 2Cl_2 \uparrow$ (the result of grinding)* Equation 1.2

$HgCl_{2\,(s)}\,(\Delta) \rightarrow HgCl_{2\,(g)} \uparrow$ (the result of heating) Equation 1.3

$AgCl_{(s)}\,(\Delta) \rightarrow AgCl_{(l)}$ (the result of heating) Equation 1.4

* Note: this equation may react separately, but the author did not mention the detail.

Fernandez-Bertran (1999) further explained that: "the milling of two solid substances generates a complex series of transformations. The mechanical energy breaks the order of the crystalline structure, producing cracks, and new surfaces. At the point of collision of the edges the solids deform and even melt, forming hot points where the molecules can reach very high vibrational excitation, and leading to bond breaking" (p581). Chemical reactions take place mainly on those broken and cracked new surfaces (Boldyrev & Avvakumov, 1971).

1.1.3 Thermal chemistry vs. mechanochemistry

The essential differences between the processes which take place on thermal treatment and on mechanical treatment are (Boldyrev & Avvakumov, 1971):

- Whether they are thermal or mechanochemical process chemical reactions involving solids take place chiefly on a surface, therefore the state of the surface plays an important role in these processes. Thermal treatment generates heat in solid and leads to the excitation of all sites in the crystal lattice, whereas by

mechanical treatment it is possible to bring only a part of the solid lattice into the excited state.

- Thermal process produces a relatively slow increase in temperature, whereas with mechanical treatment, the temperature at the points of contact solids is a rapid pulse-wise increase followed by rapid cooling (Boldyrev & Avvakumov, 1971). "These stochastic processes occur in a period of 10^{-7}s, in which thermal equilibrium does not exist." (Fernández-Bertran, 1999, p.581).

- Rather than thermal process which will potentially lead to further decomposition, mechanochemical reactions are localised, rapid processes therefore they may be quenched when the primary product is formed (Boldyrev & Avvakumov, 1971).

1.2 Classification of mechanochemistry

Mechanochemistry (mechanochemical process) as a new branch of chemical processes still does not have a well defined and commonly accepted classification. Boldyrev (1995) noted that according to Ostwald's definition mechanochemistry could be used to describe a great variety of processes including chemical reactions in shock waves, initiation of liquid explosives, acoustochemical effects in liquids and solid-state chemical reactions under mechanical loading. However recent research has been more focused on the effects of mechanical energy on the reactivity of solids. McCormic and Froes (1998) classified mechanochemical processes as: mechanical milling (MM), mechanical alloying (MA), and reaction milling (in some literature this is also called reactive milling) (RM). Suryanarayana (2001) classified the processes as mechanical alloying (MA), mechanical milling (MM) or mechanical grinding (MG) and mechanical disordering (MD). He also pointed out that some investigators use MA as a generic term, in this case MA could include both mechanical alloying and mechanical milling/disordering/reactive milling. However, recently Gacitua and Ballerini et al. (2005) claimed that mechanical alloying (MA), mechanical milling (MM) and mechanochemical synthesis (MS) are the most reasonable classifications.

Mechanochemistry Classification

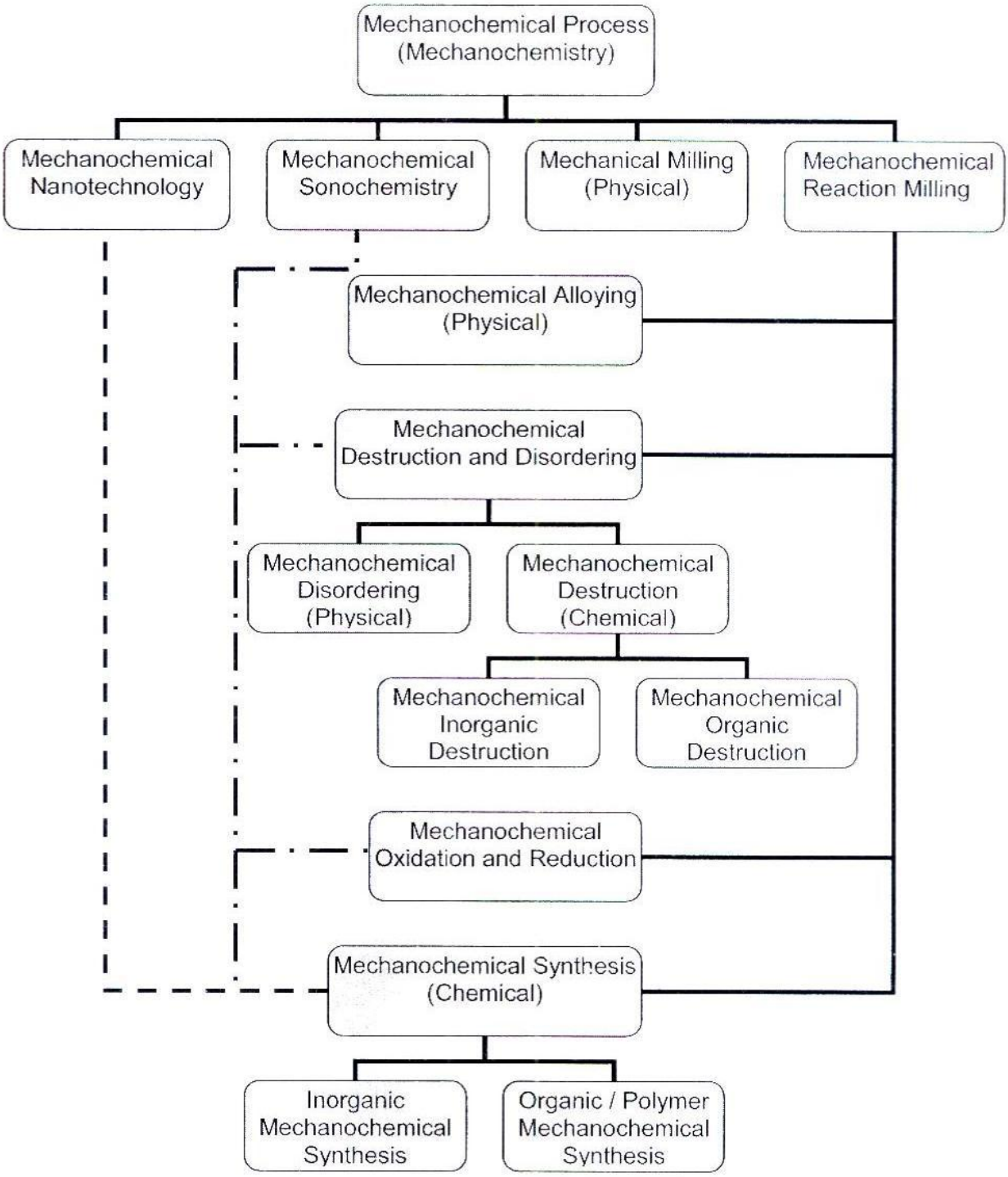

Figure 1.1 Diagram of Mechanochemistry classifications

Based on the literature, in our view the description of the processes should be based on the mechanical energy transfer method and the formation of final product. Mechanochemical processes are thus broadly classified into four types:

- Nanotechnology*.
- Sonochemistry*.
- Mechanical milling (or mechanical grinding).
- Reaction milling (or reactive milling).

*Note: sonochemistry and nanotechnology have been included for completeness but the detail of these technologies will not be discussed.

Further, mechanochemical reaction milling (reactive milling) should be classified into four sub-groups:

- Mechanical alloying,
- Mechanochemical destruction and mechanochemical disordering,
- Mechanochemical redox,
- Mechanochemical synthesis.

Mechanochemical synthesis again could be sub-grouped into inorganic mechanochemical synthesis and organic (polymer) mechanochemical synthesis.
A table summarising this scheme is given on the above page.

1.2.1 Mechanochemical nanotechnology

In a remarkable piece of work, Walch and Merkle (1998) reported they were able to position atoms and molecules in precise locations using mechanical force generated by a small robotic arm. The key point of this operation is the strength difference of the chemical bond formed between the reaction-atom with the tool molecule versus the reaction-atom with the object molecule.

The mechanism of nanotechnology is a bit like an enzyme contributing to a chemical reaction. Before the operation, the bond formed between the reactant-atom and the tool molecule is weaker than the bond which will be formed between the reactant-atom and the object molecule (target). During operation, a reactant-molecule is bound to the tip of a tool molecule at the end of the mechanical manipulator. The mechanical manipulator would be moved close to the object molecule. When the reactant-atom is close enough to the object molecule, the new bond will form and will be much stronger then the bond formed between the reactant-atom and the tool molecule. The mechanical manipulator is then twisted, the bond between the tool molecule and the

reactant-molecule will be broken, and the tool molecule can be released from the reactant-atom. The reactant-atom will firmly attach the object molecule (CRN, 2007). Thus a nanotechnology synthesis completed.

Walch and Merkle (1998) have discussed this technology in detail and they illustrated the "carbene tool added a carbon to the bridged C_2 molecule, leading to a bridged C_3 molecule perpendicular to the surface, by an overall exothermic series of steps"

Figure 1.2 Mechanosynthetic reactions

"Based on quantum chemistry by Walch and Merkle (Walch and Merkle 1998), to deposit carbon, a device moves a vinylidenecarbene along a barrier-free path to bond to a diamond (100) surface dimer, twists 90° to break a pi bond, and then pulls to cleave the remaining sigma bond" (CRN, 2007)

Nanotechnology has the potential to be an accurate and selective nanosize chemical synthesis driven by mechanical force. So here it has been included in the classification of mechanochemical process (mechanochemistry).

1.2.2 Mechanochemical Sonochemistry

Luche (1992) has discussed the detail of sonochemistry and said that the essence of sonochemistry is promoting single electrons and their transfers induced by ultrasonic waves (Luche, 1992; Beyer & Clausen-Schaumann, 2005). But Nguyen et al. (Boldyrev, 1995; Nguyen & Liang, et al., 1997; Martin & Hauke, 2005,) argued the essence of sonochemistry is cavitation, "which provides the mechanical energy for all subsequent chemical reactions, including bond scission induced by viscous frictional forces" (Nguyen & Liang, et al., 1997; p.2922). There is another review which claims that the basis of sonochemistry is free radicals formed as a result of the cavitation of microbubbles (Thompson & Doraiswamy, 1999). There was a comment in this review that "ultrasound may have other mechanical effects on a reaction, such as increasing the surface area between the reactants, accelerating dissolution, and/or renewing the surface of a solid reactant or catalyst" (Thompson & Doraiswamy, 1999, p.1215). In

the review the authors illustrated the details of ultrasound initiating chemical reactions, accelerating chemical reactions, and changing the reaction pathways.

In order to find the common characteristics of sonochemistry reactions, based on experimental data, Luche (1992) divided sonochemistry into three classes.

- The first class is constituted by homogeneous processes in solution
- The second class constitutes heterogeneous solid – liquid reactions following an ionic mechanism
- The third class of sonochemical reaction is a heterogeneous system which can follow a SET (single electron transfer) mechanism when subject to mechanical and chemical roles of sonication.

Boldyrev (1995) compared mechanochemical reactions (mechanochemical reaction milling) with ultrasonic chemical reactions including reaction site, reaction temperature and reaction occupied space. Generally, ultrasonic chemical reaction could be described as ultrasound promoting the size and structure reduction coupled with oxidation – reduction and chemical synthesis (Thompson & Doraiswamy, 1999). Hence sonochemistry is a branch of chemistry where chemical reactions are driven by a mechanical source (ultrasound) and as a result we have included it in mechanochemistry.

1.2.3 Mechanical milling (MM)

According to McCormick and Froes' definition (1998), mechanical milling refers to "the milling of a pure metal or compound that is in a state of thermodynamic equilibrium at the start of milling" (p.61). Mechanical milling (MM) is often used in preparing mixtures of nanosized grains of different phases which include nanocrystalline phases of elements or of pre-alloyed materials prepared by conventional alloying methods (Dunlap, 2000).

1.2.4 Mechanochemical Reaction milling (RM)

Mechanochemical reaction milling is a massive, unselective chemical reaction driven by mechanical force. McCormick and Froes defined reaction milling as "using mechanical processing to induce chemical reactions" (McCormick & Froes, 1998, p.61). Following this definition, reaction milling will result in some chemical change

such as electron transfer or sharing which forms new chemical bonds and therefore produces new chemical products other than the reactants. In some literature, reaction milling is also referred to as “reactive milling”.

Unlike gases and liquids, mechanochemical processing (which deals mainly with solid reactants) supports collision and shear strains that are able to trigger chemical reaction. Collision and shear is more effective in stimulating reactions than simple isotropic compression (Boldyrev & Tkácová, 2000).

The two essential features that seem to drive mechanochemical reactions are the increasing the number of particles and the increase of contact area due to plastic deformation of one component or both (Boldyrev & Tkácová, 2000).

Hasegawa (1995) reported that the specific surface area would increase with milling time. Depending on the different type of milling matrix, there is an increase of between 30 to 500 times surface area after 30 hours milling. (of course except the milling time, the surface area increase relies on the Hardgove index of milling matrix and milling media). Gilman (1996) commented “Sheared spheres become ellipsoids, cubic symmetry becomes tetragonal, and so on. Such symmetry breaking destabilizes the electronic structure of bonding and makes the solid prone to chemical reaction. Such mechanochemical phenomena are found in a variety of processes - friction and wear, detonations, solid-state synthesis and mechanical alloying.” (p.65).

Murtyand and Ranganathan (1998) suggested that fragmentation and coalescence events could happen during ball to powder collisions. During mechanical milling (as next page) only fragmentation or part fragmentation events occur, but for reaction milling, fragmentation and coalescence events both exist

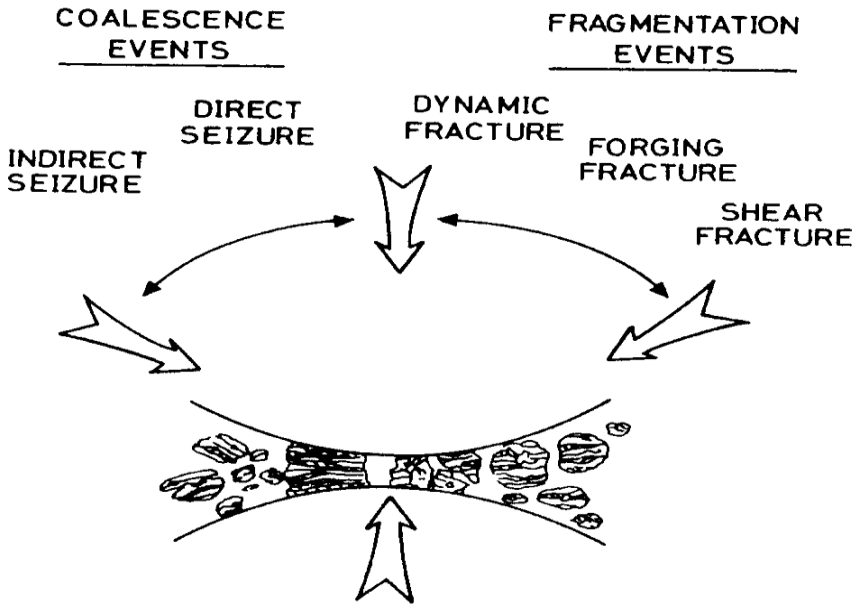

Figure 1.3 Schematic of events occurring during ball to powder collision (Murty and Ranganathan, 1998)

1.2.4.1 Mechanochemical Process in Cold Alloying (MA)

Mechanical alloying specifically refers to the formation of alloys from elemental precursors during processing in a ball mill (McCormick & Froes, 1998). It can be described as a process, used to obtain a homogeneous alloy. Powders (of different metals or alloys / compounds) are mixed and milled together; material transfer within reactants is involved (Suryanarayana, 2001).

An alloying process is not a simply metals physically mixing and blending. Alloys could be homogeneous substitutionally or interstitial solid solutions. In an alloy either the atoms of one metal are distributed randomly among the other or have a definite composition and internal structure (Shriver, 1996). The mechanochemical alloying process is certainly this type of synthesis but (because they are metals) without the obvious electron sharing and general chemical bond forming. Thus mechanochemical alloying has been included in mechanochemical reaction milling.

Around 1966 Benjamin (1970) and his co-workers developed the processing technique which blended elemental powder mixtures and allowed production of homogeneous alloy materials (Suryanarayana & Ivanov et al., 2001; Locci & Orru et

al., 2006).Since then a huge amount of work has been done on mechanochemical alloying of almost all metallic elements. In 1983 Schwarz and Johnson (1983) demonstrated the solid-state amorphization reaction for amorphous alloys and in the same year another novel technique for producing amorphous alloy powders by mechanical alloying (MA) was reported by Koch and Cavin et al. (1983). Since then, MA production of amorphous alloys has become widely accepted (El-Eskandarany & Aoki et al., 1990).

It should be emphasised that in order to form a new alloy compound, milling process should mix at least two or more different simple metallic alloys or compounds. For example Fe-M (M = Al, Si, Cu) nanocrystalline mechanical alloying (Kuhrt, 1993), Pb-Al binary system mechanically alloyed by high energy ball milling (Zhu & Che et al., 1998), Fe-V, Fe-Cr, Fe-Mn alloys produced by mixing metal elemental powder by high-energy ball milling (Caër & Ziller et al., 2000).

Plastic deformation predominates in a typical metal mechanochemical alloying process (Senna, 2001). Dunlap (2000) divided mechanochemical alloy process into five steps:

a. Plastic deformation
b. Welding predominance
c. Welding-fracture equilibrium
d. Random lamellae orientation
e. Micro-structural refinement

These five steps tend to describe the mechanism of the mechanochemical alloy process.

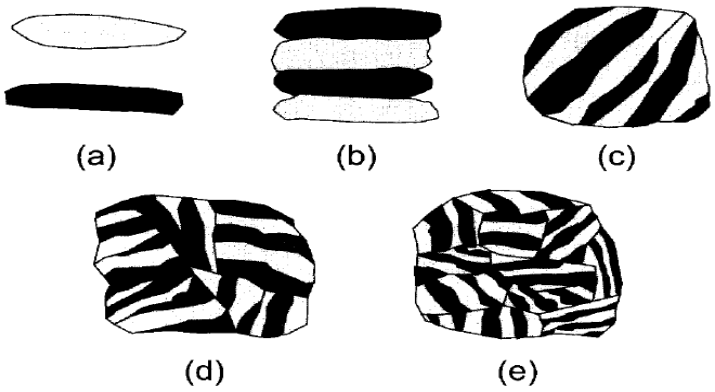

Figure 1.4 The five stage of mechanical alloying. (Dunlap, 2000).

Oxides are generally much more brittle than metals. However, in 1980 Senna (2001) and a reference there in (a thesis result by W.Hess) noted that in a small area or in a small particle, brittle materials deform themselves plastically and form "alloys". This remarkable result means that during the mechanochemical processing, after particle size is reduced, most of reactants will show some degree of plastic behaviour. Hence these five steps of the milling mechanism should not only be applied in mechanochemical alloying but can also be applied to most reactants during the mechanochemical process, especially in mechanochemical synthesis. In other words, these five steps could be applied in both ductile and brittle reactants during mechanochemical treatment.

1.2.4.2 Mechanochemical destruction and disordering (MD)

- Mechanochemical disordering

In his book Suryanarayana (2001) defined mechanochemical disordering (MD) as the destruction of long-range order to produce either a disordered or an amorphous phase and gave a number of examples.

- Mechanochemical destruction

That silver and mercury solid salts could be decomposed by milling was known as early as the19^{th} century (refer to equations 1.2 and 1.3). Based on this, the concept of mechanochemical milling decomposing inorganic substances by milling was established (Boldyrev & Avvakumov, 1971) and some research has been done for instance TiB_2 and TiB_2/FeB Produced from ilmenite (iron titanate) (Millet & Hwang, 1996).

Boldyrev and Avvakumov (1971) have reviewed the process of inorganic compounds mechanochemically decomposing including carbonated metal, alkali metal, alkaline earth metal and rare earth metal nitrates.

In the last few decades, especially starting from the 1990's, organic material mechanochemical destruction has been developed and been widely used in hazardous organic material reduction and hazardous polyhalogenated material dehalogenation (Field et al., 1997)

1.2.4.3 Mechanochemical oxidation – reduction (redox)

Typical mechanochemical redox reactions use one element (usually a metal or semi-metal) to replace another element (usually another metal element) from a composite. For example silicon replaces copper from copper oxide, and silicon replaces nickel from nickel oxide (Xi & Zhou et al., 1996; Corrias & Paschina et al., 1997; Corrias & Paschina et al., 1998) e.g.:

$$2NiO + Si \rightarrow 2Ni + SiO_2 \qquad \text{Equation 1.5}$$

$$2CuO + Si \rightarrow 2Cu + SiO_2 \qquad \text{Equation 1.6}$$

These reaction are not limited to metal - however, Chen, Ninham and Ogarev (1995) demonstrated the replacement of oxygen by gaseous N_2 in SiO_2 -- a metal-gas reaction.

$$3SiO_2 + 4N_2 \rightarrow 2\ \alpha\text{-}Si_3N_4 + 3O_2 \qquad \text{Equation 1.7}$$

Replacement reactions are not limited to simple replacement of elements, other types of redox reaction start from two different composites and lead to more complex final products.

1.2.4.4 Mechanochemical Synthesis

Mechanochemical synthesis is considered as a chemical reaction during the mechanochemical process where reactants (of different chemical compounds or elements) are mixed and milled together, electrons transferred or shared within the reactants and new chemical bonds are formed.

As mentioned earlier, in the initial stage of mechanochemical synthesis, particle size reduction and plastic deformation occurs at least to some extent before the chemical bonds are formed. For such reactions, consider the reduction of particle - quartz dimensions on size could be divided into three stages (Boldyrev & Avvakumov, 1971).

1. The first stage is characterised by a progressive decrease with milling time of the quartz particle dimensions.
2. The second stage is characterised by the start of aggregation of the particles.
3. The third stage is characterised the establishment of an equilibrium, in which the quartz dimensions remain generally unchanged with time. The specific surface area changes analogously.

There appears to be an important feature here. As the particle size is reduced, there is also an increase in plastic deformation of particles. Thus during milling, the surface area not only increases but the surface contact is enhanced by the deformation of the particles. Boldyrevand and Tkácová (2000) have pointed out that plastic deformation of one component or both with the increasing of contact area is more important than the number of particles.

As noted above, research has shown that both brittle and ductile particles will show plastic behaviour. Hess found there was a critical size range by determining stress-strain curves of compressed single particles with different sizes (Senna 2001). Perhaps not surprisingly, the size at which plastic deformation and "alloying" occurs decreases as the materials become harder. (see sections 3.7 and 3.8).

Boldyrev (1995) showed it takes about 10^{-3} s to formed a stress field in ionic crystals, but it may take many hours to relax the elastic stresses due to the formation and motion of point defects. Boldyrev emphasised that it may take even longer for a transition from a metastable amorphous state into a stable crystalline form to occur. Therefore the mechanism of mechanochemical synthesis using either brittle or ductile components could be understood to be similar to plastic deformation in metallic alloys. The only difference between brittle and ductile components is their particle size of plastic deformation during milling and the point at which plastic deformation becomes significant. As well as that Senna (2001) also pointed out that the chemical reaction is not a direct result of plastic deformation itself. Plastic deformation of the reactants would cause an increase in the number of low coordinate atoms which could, in turn, promote chemical reactions.

- Some examples of inorganic mechanochemical synthesis.

Typical mechanochemical synthesis is $LiTiO_2$ synthesis from LiO_2 milling with TiO_2; $LiFeO_2$ produced from LiO_2 milling with Fe_2O_3; and $Li_xMn_{(1-x)}O$ generated from Li_2O plus MnO_2 (Obrovac & Mao et al., 1998).

$$½\ Li_2O + ¾TiO_2 + ¼Ti \rightarrow LiTiO_2 \qquad \text{Equation 1.8}$$

$$Li_2O + Fe_2O_3 \rightarrow 2LiFeO_2 \qquad \text{Equation 1.9}$$

$$X½Li_2\ O + (½ - ¼X)MnO_2 + (½ - ¾X)Mn \rightarrow Li_x\ Mn_{(1-x)}\ O \qquad \text{Equation 1.10}$$

A synthetic preparation of zircon and its mechanism by milling monoclinic zirconia with precipitated silica was studied by Puclin and Kaczmarek (1997). They showed that synthesis of zircon by component oxides using mechanical processing in laboratory is possible, ie.

$$\text{Amorphous phase} \rightarrow t\text{-}ZrO_2 + SiO_2 \rightarrow ZrSiO_4 \qquad \text{Equation 1.11}$$

More recently in 2000, the mineral $La_{4.67}(SiO_4)_3O$ was synthesised by Tzvetkov and Minkova (2000) while milling SiO_2 with La_2O_3 and in recently Apatite-type lanthanum silicates have been successfully prepared at room temperature by dry milling hexagonal $A{-}La_2O_3$ with either amorphous or low cristobalite SiO_2 (Fuentes, Rodríguez-Reyna et al., 2006).

When more than two different metal-oxygen bonds are involved in a reaction, there is almost always a possibility of acid/base reactions. A surface metal-oxygen bond can behave as either acidic or basic depending on the exact direction of electron shifts during cleavage. As a result, there are occasions when a reaction could be considered a reaction between a Lewis acid and a Lewis base and the final product is a salt. Mamoru estimated that there is a possibility for Lewis acid/base reactions to occur in a system containing only one metallic species (Senna, 2001).

It should be pointed out at this stage that mechanochemical synthesis is not restricted to inorganic systems. Organic compounds have been shown to also undergo similar mechanochemical reactions (see below)

- Organic and polymer mechanochemical synthesis (mechanochemical polymerization)

There is no meaningful line between mechanochemical inorganic synthesis and mechanochemical organic synthesis. Here, mechanochemical organic synthesis refers to those final chemical compounds that contain carbon chain. In some literature, for those final product is long carbon molecule chains, the concept of polymer mechanochemical synthesis is used, and in other literature the concept of mechanochemical polymerization is used instead of mechanochemical polymer synthesis.

Hasegawa and Akiho et. al (1995) have discussed the relationship between polymerization and grinding. They noted that "Mechanochemical polymerization seems to be one of the most promising processes for the production of composite materials of inorganic compound and organic polymers" (p.297). Because of some inherent advantages during the processing, mechanochemical polymer synthesis such as "excellent versatility, scalability and cost-effectiveness", the high-energy ball milling techniques should be considered well suited for large quantity of polymer mechanochemical synthesis (Gacitua & Ballerini et al., 2005). It was reported that this method could be used in polymeric pro-drug development (Kondo & Kuzuya et al., 2002). The concept here is to produce an inactive polymeric form of a drug that is converted into an active form in the body by a chemical reaction in the digestive tract.

Smith and Ade et al. (2000) reported the preparation of a polymer alloy from poly(methyl methacrylate) with polyisoprene and poly(ethylene-alt-propylene). They proposed that in the initial stage of milling, polymer particles will be crushed to powder where not only the physical size is reduced but different polymer components are distributed evenly in the milling system. Since polymers should be considered as fairly ductile reactants compared to oxides and metals, they should show significant plastic behaviour, and therefore there is a distinct possibility for those polymer reactants to show similar plastic deformation stages as those seen in mechanical alloying (Dunlap, 2000). The deformation stage would clearly increase the contact of reactants and enhance bonding and cross-linking opportunities.

The second stage, where size reduced polymers sustained shear, extension, fracture and cold welding, is expected to induce chain scission or hydrogen abstraction, hence resulting in molecular weight reduction and free radical formation. The authors further noted that for those broken chains of the same polymer species, the reaction of free radicals will affect the polymer miscibility and coalescence kinetics. However for those broken chains of different polymer species, under the right set of conditions, reaction of free radicals could produce block or graft copolymers as compatibilizing agents.

The details of chemical bonds changing during polymerisation and cross-linking have also been discussed by Sohma (1989), Martin and Hauke (2005).

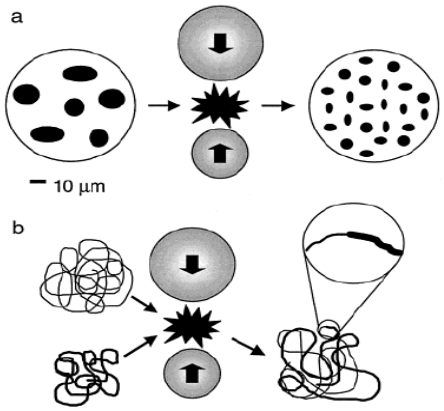

Figure 1.5 "Schematic illustration showing the possible effects of solid-state mechanical alloying on polymer blends. In part a, high-energy impact between ball bearings promotes a physical reduction in the size scale of the blended polymers. Another effect is shown in part b, in which free radicals generated by chain scission chemically couple polymer chains and produce a more stable blend" (Smith & Ade et al., 2000, p.2596).

1.2.4.5 Mechanochemical reaction milling dynamic equilibrium

The dynamic equilibrium here only discusses the mechanochemical reaction milling. Some of previous research showed that the reactions taking place on mechanical treatment are reversible. For example, treatment of zinc oxide in the presence of carbon dioxide leads to the formation of zinc carbonate, whereas dissociation of zinc carbonate takes place on treatment in a vacuum (Boldyrev & Avvakumov, 1971).

They commented that “if the rates of the forward and reverse reaction on mechanical treatment are equal, there is no overall macroscopic change in the system.” (p.854)

1.3 Mechanochemistry applied to environment issues

Traditional industrial disposal treatment methods can be divided into three types: destructive oxidization, decomposition and burial. For organic disposal, destructive oxidization and decomposition methods are usually used and for inorganic disposal burial is often the only viable option.

Because it can destroy a range of organic and inorganic substances, mechanochemical processing offers a relatively inexpensive, environmentally friendly method of dealing with polluted soil and similar solids

1.3.1 Mechanochemistry applied in organic pollution – mechanochemical destruction

1.3.1.1 Traditional organic disposal treatment method

Organic disposal treatment methods can be divided into thermal, chemical biological and photochemical methods (Bellingham, 2006; Li, 2006). Thermal treatment methods use air to oxidize organic material to principally carbon dioxide, water and an inorganic residue. Chemical treatment methods use chemical reagents to oxidize organic material. Biological and photochemical methods use microbes or sunlight to oxidize organic material to (usually) the same products as thermal treatments. All these methods have their advantages and disadvantages.

Thermal methods have high energy consumption, high capital cost of plant and equipment and need extensive safety controls to be efficient. Chemical methods can have low reaction rates, low throughputs, are expensive and often a highly reactive reagent is involved but generally the process is easier to control. However, Rowland and Hall et. al (1994) comments that “high temperature chemical reactions can be accompanied by unwanted toxic emissions or by products which may involve unacceptable risks to the environment” (p.223). Biological methods are slow and

concentration restricted (Bellingham, 2006). In fact the most widely used methods (thermal and burial) are not very environmentally friendly.

1.3.1.2 Organic disposal using mechanochemical destruction

Research on the mechanochemical decomposition of organic material such as DDT, PAH, Hydrocarbon, has been done since the 1990's.

In 1994 an article, "Destruction of Toxic materials" (Rowlands & Hall et al., 1994), was published in Nature Journal in the Scientific Correspondence section in Australia. The authors observed that they "have developed a low-temperature method involving mechanochemical reactions induced by mechanically milling the toxic material with a suitable reactant in a closed vessel. Such reactants may include reactants which break down the entire molecule or react selectively to remove chlorine." (p.223). This article should be considered as a milestone in applied mechanochemistry in dealing with environmental issues.

Field and Sternhell et al. (1997) have carried out a number of investigations with biphenyl, naphthalene, anthracene and phenanthrene in mechanochemistry and discovered that with apparently non-reactive matrices (alumina and silica), aromatic hydrocarbons treated mechanically were destroyed and converted to carbon (as graphite) and a variety of partly hydrogenated materials. They also discovered that silica is a more effective medium in the destruction of organic material compared to alumina but oxygen slows down the rate of reactions.

In order to explore the mechanism of the destruction of aromatic hydrocarbons, Li (2006) investigated the reaction of polycyclic aromatic hydrocarbons, including simple polycyclic aromatic compounds such as naphthalene, anthracene and chlorinated polycyclic aromatic compounds like chloronaphthalene, bromonaphthalene etc. She found the mechanochemical decomposition process is a very effective way to destroy these PAHs.

Bellingham (2006) reported over 500 mechanochemical destruction experiments including milling of DDT, DDD, DDE, Dieldrin, hexachlorobenzene, pentachlorophenol, naphthalene and several other organic compounds -- conducted

using laboratory, pilot and full scale ball mills. By gas chromatography mass spectrometry and other analytical techniques he determined that mechanochemical destruction of the above mentioned organic compounds was achieved. Destruction efficiencies for a number of organic compounds were greater than 99%. He also developed an appropriate mechanochemical process method for the destruction of organic pesticide compounds. One significant point emerging from this work was the inability to account for all the chlorine from the chlorinated hydrocarbons.

It was assumed that the organic chlorine would form (inorganic) chloride which would be easily leached with water from the reaction and quantified. It was found, however, that even exhaustive extraction with boiling water (chloride is very soluble in water) could only recover 50-60% of the expected chlorine as chloride. Further experiments where NaCl was milled with quartz showed similar discrepancies. XRF analysis for chloride gave an essentially quantitative result. So it was concluded that the chloride was firmly trapped or bound into the quartz matrix. Subsequent trials also suggested that other elements could be similarly trapped.

1.3.2 Mechanochemistry applied in toxic metal pollution and mechanochemical synthesis

1.3.2.1 Metal contamination in the environment

There are two major source of heavy metals existing in the environment; one is naturally exists, for example, rock weathering within the catchments, and another source is come from human activities (Dickinson & Dunbar et al., 1996). Certain trace amounts of heavy metals, including cobalt, copper, manganese, molybdenum, vanadium, strontium, and zinc are necessary for living organisms including human being, but would be harmful if these heavy metal exceeded the required levels. Other heavy metals such as mercury, lead and cadmium not only have no known beneficial effects but accumulate in organisms over time and can cause serious illness (Wikipedia, 2007).

New Zealand used to be considered a clean environment (McLay, 1976), but various researchers have shown that New Zealand's environment suffers from problems similar to other countries. For example researches on the water around Auckland and

Wellington have shown that heavy metal contamination is everywhere (Stoffers & Glasby et al., 1986; Deely & Tunnicliff et al., 1992; Abrahim & Parker 2002).

It was reported that Cd, Cu, Pb, and Zn were the most common metal pollutants found in New Zealand, and these elements are concentrated in the upper part of the sediment cores as compared to lower concentrations found deeper (older, pre-industrial) sediments (Stoffers et al., 1986; Deely et al., 1992).

Heavy metal contamination in localised areas localised adjacent to drains is mainly influenced by industrial activity (Stoffers et al., 1986; Deely et al., 1992; Abrahim, 2002).

1.3.2.2 Metal (Inorganic disposal) mechanochemical synthesis

It was suggested as early as 1971 that mechanochemical technology could be used in the production of binding agents for industrial wastes (Boldyrev & Avvakumov, 1971). The idea that mechanochemical processes can be used in the synthesis of metal elements from silicon dioxide and various metal oxides or carbonates leads to a potential method for dealing with inorganic industrial disposal. Bellingham's result (Bellingham 2006) confirmed the findings of others (Boldyrev & Avvakumov, 1971).

If mechanochemistry could be used to deal with inorganic pollution by binding the metals in some way to an insoluble matrix like quartz at the same time as the organic components are being destroyed, the potential for dealing with industrial waste disposal is huge.

Chapter 2. Experimental method

2.1 Parameters influence milling results

In a defined mechanical reaction system, among various possible paths, the conditions of milling (milling parameters) are of crucial important in determining the solid state reaction type (Padella & Paradiso et al., 1991).

2.1.1 Type of milling machine

- High energy ball milling

High energy ball milling is where the energy transfer to the powder particle is by a combination of shearing action and impact of the high velocity balls with the powder (Murty & Ranganathan, 1998). The energy transfer is "based on the repeated occurrence of single impact events where powder particles are trapped and cold-worked" (Delogu & Deidda et al. 2004, p.5121). Murty and Ranganathan (1998) characterised the high energy ball mill as "repeated welding and fracturing of the powder" (p.104). During the high energy ball milling process, deformation, breaking and cold welding of powder particles are continuously repeated and particles of the brittle powder will be broken into fine particles(Zhao & Zwick et al. 2003).

The type of high energy ball milling machine used, depends on the purpose. Some are designed for laboratory uses and some are designed for production uses. Generally, the difference is between their capacity, efficiency of milling and additional arrangements for cooling, heating, etc. Mills can be described as shaker mills, planetary ball mills, attritor mills, horizontal ball mills, vibratory ball mills and commercial production-size ball mills (Dunlap, 2000; Suryanarayana, 2001). Mechanical reaction is usually carried out in high energy ball mills such as vibratory mills, planetary mills and attritor mills (Murty & Ranganathan, 1998). In this research a Retsch PM-100 planetary ball mill was used.

- Planetary ball mills

The planetary ball mill is one type of high energy ball mill. The milling jar is arranged eccentrically on a sun wheel of the planetary ball mill, with the direction of the rotation of the sun wheel being opposite to that of the milling jar (Retsch, 2006).

The following diagram illustrates the arrangement:

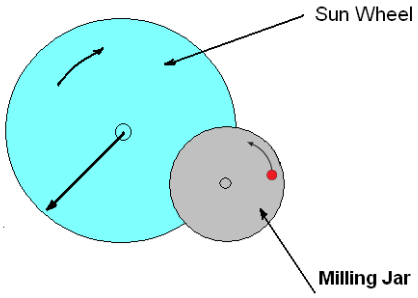

Figure 1.6 Schematic depicting the PM100 milling jar work with the sun wheel -- modified from "Retsch GmbH" user's guide (2006)

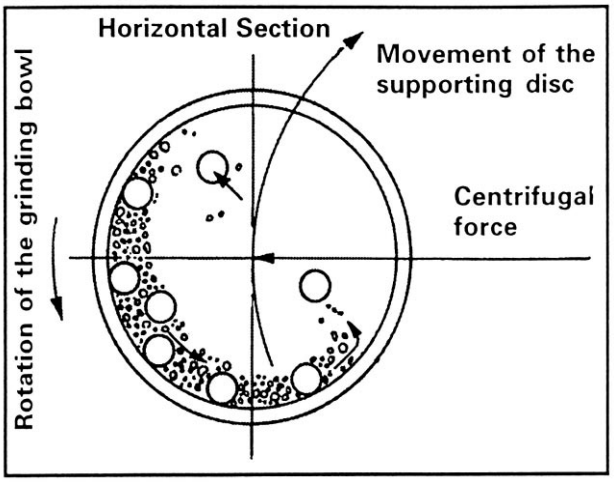

Figure 1.7 Schematic depicting the ball motion inside the ball mill – together with the motion components of both the supporting disk and the jar, rotating along different axes in opposite directions. (Suryanarayana, 2001; Delogu & Orru et al., 2003)

In this type of mill, the centrifugal forces alternately act in opposite directions to not only prevent milling balls from being pinned to the inside wall of the jar but the force also causes the milling balls to run down the inside wall. This creates a friction grinding effect followed by the balls lifting off and flying to the other side of the jar where they collide and provide impact grinding effects (Suryanarayana, 2001).

The difference in speeds between the balls and milling jars produces an interaction between frictional and impact forces. The interplay between centrifugal forces together with milling ball collision and friction releases high dynamic energies. These forces produce a high and very effective degree of size reduction, as they increase powder surface area (Boldyrev & Avvakumov, 1971).

While only dry milling was used in this study, slurries of solids in various liquids are commonly milled to control particle size and other factors (Suryanarayana, 2001). Bellingham (2006) noted that slurries of DDT in water also resulted in the destruction of DDT.

2.1.2 Milling time

Milling time is one of the most important parameters. The milling time largely depends on the type of mill used and the intensity of milling (milling speed). Yamada and Koch (1993) reported that 20 minutes of milling in a SPEX mill is equivalent to 20 hours of milling in the type of INVICTA BX 920 low-energy mill. Meanwhile milling time also depends on ball to powder mass ratio (BPR). Higher BPR normally results in less milling time. Suryanarayana (2001) suggested that the milling time should be chosen so as to achieve a steady state between the fracturing and cold welding of the powder particles. He further warned that some of undesirable contamination and phases may form with an unreasonably long milling time. Hong and Bansal et al. (1994) believed that for all milling temperatures, 48 hours of milling time is more than sufficient to achieve a steady state of the microstructure.

2.1.3 Ball size

Both ball size and ball material will influence milling result. The density of milling ball is related to the impact forces on the powder. It is considered that relatively large size and weight of the milling balls will transfer more impact energy to powder particles (Suryanarayana, 2001).

2.1.4 Ball to powder mass ratio

Ball to powder mass ratio influences the grading result. Since it will not only influence the milling energy input but also the milling processing time, balls to the powder mass ratio (BPR) should be considered as one of the most important variables in the milling process. In some literature this is also referred to as charge ratio (CR). This figure can vary from 1:1 (Chin & Perng, 1996) to 220:1 (Kis-Varga & Beke, 1995) through different research projects and different researcher. Where a small capacity mill such as a SPEX mill is used, Suryanarayana (2001) suggested that a ratio of 10:1 was an optimum and in a large mill such as in an attritor, a higher BPR of up to 50:1 or even 100:1 could be used.

Usually a higher BPR results in less milling time. Gerasimov and Gusev et. al. (1991) noted that the structure of the product in mechanical alloying depends on both the elemental composition and the milling conditions. They demonstrated that a lower BPR ratio with lower milling speed results in meta-stable phases while higher a BPR with higher milling speed results in equilibrium crystalline products. Suryanarayana et. al. (1992) reported that during their research project, Ti-33at% Al powder mixture milled in a SPEX mill for 7 hours at a BPR of 10:1 is equivalent to 2 hours at a BPR of 50:1 and 1 hour only if at a BPR of 100:1. Suryanarayana (2001) concluded that at a high BPR and with an increase in the weight proportion of the balls, the number of collisions per unit time increases and consequently more energy is transferred to the powder particles which results in alloying taking place faster.

2.1.5 Milling speed and temperature

Different milling speeds may result in different product. Originally it was thought that the faster the milling speed, the higher energy input into the powder, but Suryanarayana (2001) suggested that depending on the design of the mill, there should be certain limitations to the maximum milling speed able be employed. This maximum speed should be just below a critical value so that the balls could fall down from the maximum height to produce the maximum collision energy. He further explained that if milling above a critical speed in a conventional ball mill, the balls will be pinned to the inner walls of the jar and will not fall down to exert any impact force. Calka and NIkolov et al. (1993) also reported that different level of energy input during milling may result different final product with different constitution and/or structure.

Suryanarayana (2001) also mentioned that in a paper report of Kaloshkin et al., high milling speed may lead to high temperatures. While it is an advantage in some cases where diffusion is required to promote homogenization and/or alloying in the powders, the increased temperature accelerates the transformation process and results in the decomposition of supersaturated solid solutions or other metastable phases formed during milling. In this case the increasing temperature may become a disadvantage. So a limit to the maximum speed (or intensity of milling) is often necessary.

Temperature changes during milling will influence the thermochemical balance and further influence the milled product and, to a large extent the nature of phase transitions during milling is a function of the temperature of milling (Hong & Bansal et al., 1994; Murty & Ranganathan, 1998).

Based on a serial of investigation of the intentionally varied temperature in milling, Suryanarayana (2001) concluded that most of the temperature rise is generated by shearing between the powder particles and balls. The temperature is in the range from 100^{o}C to 120^{o}C. He also emphasised that this is a macroscopic temperature rising range, where the local (microscopic) temperature can often exceeding the melting points of some of the component metals. On the other hand, Kwon & Gerasimov et al. (2002) reported that after 20 minutes of highest intensity milling, temperatures of the balls could reach over 600^{o}C. Takacs and McHenry (2006) suggested that ball temperature against milling time should fitted an exponential approach to a steady state. They concluded that "the impulsive temperature increase of the powder compressed between the colliding milling tools may add an additional 50^{o}C - 300^{o}C to give the highest local temperature" (p.5246). The variations in conclusions suggested that the exact cause of the temperature rise during milling is still uncertain.

2.2 Milling condition

2.2.1 The mill

In this research a Retsch PM100 single-station ball mill was used. The PM-100 handles milling jars from 50 – 500 mL in size. In this study a 500 mL chrome steel milling jar with carbon steel milling balls and a 50 mL zirconia ceramic jar with zirconia milling balls were used.

Figure 2.1 Retsch GmbH planetary ball mill PM100 (Retsch, 2006)

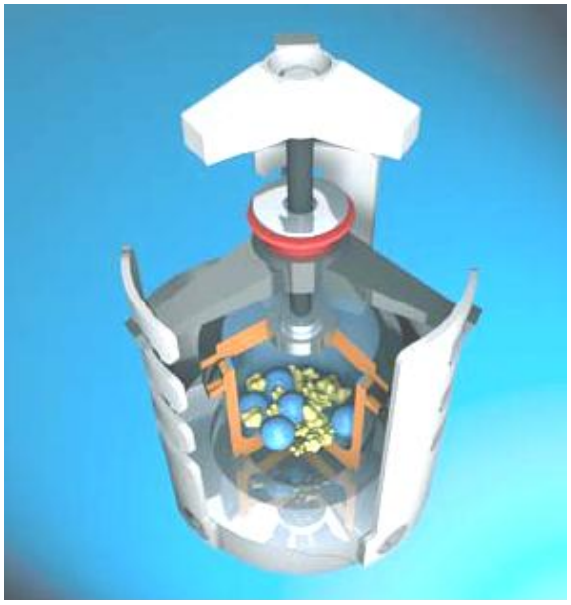

Figure 2.2 Structure of Milling jar (Retsch, 2006)

2.2.2 Milling parameters used in this research

- Milling times

Milling times ranged from 5 minutes to up to 160 hours.

- Ball size

In the 500 mL steel jar, 20 Steel balls with average 15mm in diameter were used. In the 50 mL zirconia jar, two 20 mm zirconia balls were used.

- Ball to powder mass ratio

In this research, a 5:1 of BPR (milling ball vs. metal oxides plus silica) ratio was used in the steel milling system (steel milling jar with steel milling balls) and 10:1 of BPR was used in zirconia jar and balls unless specified.

- Milling speed and temperature

500 rpm speed was used in all experiments in this research. It is just below the maxim milling speed recommended by supplier. It is believed that this speed is able to achieve nearly maximum energy transfer but avoid balls being pinned to the inner walls of the jar and the temperature was kept in the 100 – 120^{o}C range. Temperatures were measured immediately after milling motor stopped by opening the jar and inserting a mercury thermometer.

2.2.3 Milling method used in this research

All samples were prepared from dry powdered reagents and quartz sand using the following two methods:

2.2.3.1 Using the 500 mL chrome steel jar

Unless specified, for specimen milled in chrome steel milling jar, the milling procedure was carried as:

1. About 0.5 gram metal-oxide powder was weighed;
2. Silica was added up to 50 gram;
3. All the sample was carefully transferred into the chrome steel milling vessel and milled for 5 minutes;
4. A sample of 2 grams was taken for retention;
5. Milling was continued and 2 gram samples were taken in each interval for retention;
6. A 1.0 gram sample was accurately measured from the retention sample into a 250 mL beaker for EPA3050B digestion
7. AA / ICP analysis

2.2.3.2 Using the 50 mL zirconia jar*

Unless specified, for milling in the zirconia milling jar, the milling procedure was carried out as follows:

1. About 0.05 gram metal-oxide powder was weighed;
2. Silica was added -- up to 5 gram;
3. All the sample was carefully transferred into the zirconia milling vessel and milled for 5 minutes;
4. About 2 grams of sample was taken for analysis;
5. Milling was continued until 1 hour was up;
6. The rest (about 3 grams) of the sample powder was removed and put into a test tube for retention,
7. Step (1) to (6) were repeated for the 2 hour, 3 hour and 4 hour samples;
8. A 1.0 gram sample was accurately measured from the retention sample into a 250 mL beaker for EPA3050B digestion

* note: zirconia ceramics (ZrO_2) - ceramics of this type contain a small amount of yttrium oxide as a stabilizer.

2.2.4 Metal elements contained in milling jar and balls

For the trace metal elements contained in the steel milling balls, chrome steel milling jar and zirconia milling media, see appendix 4.

2.3 The silica sand (quartz) milling matrix used in this research

In this research, silica sand (obtained from ACI Glass) was used as the milling matrix. It was identified (microscopically) as almost entirely composed of slightly worn crystalline quartz (SiO_2) grains, typical of "pure" silica sand.

2.3.1 Size of silica sand

The silica sand size was measured by sieve analysis (Standard Endicot Sieves), Sand and milled material was measured by laser scattering particle size analysis using a Mastersizer 2000 (Malvern Instruments Ltd) see Figure 3.7-1.

The following table shows the weight percentage of size distribution of raw silica sand by sieve analysis.

Silica sand size: (um)	percentage
between 150um - 300um	84%
between 300um - 600um	12.5%
between 106um - 150um	3%
less than 106um	0.5%

Table 2.1 The size distribution of silica sand

2.3.2 Metals contained in the quartz

Extractable chromium, copper, iron, lead, magnesium, sodium, zinc contained in the silica was checked by the EPA3050B method and HF digestion. Since the raw quartz (84% of silica sand is between 150um - 300um) does not easily react with HF, following the Nanjing Fibber-glass Research and Design Institute method, the quartz was milled for 1 hour in the zirconia milling jar.

The EPA 3050B digestion was compared for unmilled and milled quartz. Statistical analysis (2-sample T test) showed that by EPA3050B digestion there is no significant difference for all seven elements in SiO_2 (Cr, Cu, Fe, Mg, Na, Pb and Zn) between un-milled quartz and one hour milled quartz in the zirconia jar (see the appendix – 6). The following table (Table 3.1) compares the average of detected trace metal elements in unmilled quartz and milled quartz by EPA 3050B digestion method and by HF digestion of the residue (for details and standard deviation see appendix – 5):

Metal (ppm)	Average Cr	Average Cu	Average Fe	Average Mg	Average Pb	Average Zn	Average Na
in unmilled SiO_2 by EPA3050B	8	2	60	6	1	53	117
in milled SiO_2 by EPA3050B	5	1	77	10	0	41	154
in milled SiO_2 by HF digestion of the residue	12	5	171	25	1	9	91
Sum in milled SiO_2 (EPA3050B + HF digestion of the residue)	18	6	249	34	1	50	245

Table 2.2 Average metal concentration in unmilled and 1 hour (zirconia jar) milled quartz

2.4 Digestion methods

2.4.1 The EPA 3050B digestion method

Environmental Protect Agency Testing Method 3050B (Acid Digestion of Sediments, Sludge and Soils) (US.EPA, 2003) was selected for the sample digestion after milling.

This is a very strong acid digestion method that will dissolve almost all elements that could become "environmentally available". However, this method is not a total digestion technique for most samples, as stated in the beginning of the method "By design, elements bonded in silicate structures are not normally dissolved by this procedure as they are not usually mobile in the environment." (US.EPA 2003, 3050B) This is an important point when considering the hazard associated with contaminated minerals and soils. If the contaminants are not mobile they usually have little environmental impact.

2.4.2 Second and third digestion by EPA 3050B method

1. EPA3050B digested residue (as much as possible) was carefully removed from filter paper into a weighed 400 mL beaker;
2. The transferred residue was accurately weighed;
3. The filter paper was fold into a platinum crucible;
4. The platinum crucible was covered, then the filter paper was ashed in it;
5. Then the platinum crucible was transferred into the furnace;
6. The crucible contents were ashed in furnace at 650^{o}C for 30 minutes;
7. The platinum crucible was cooled down to room temperature;
8. The residue was transferred into above weighed 400 mL beaker and the mass of the ash was calculated;
9. The residue was accurately weighed again;
10. The EPA 3050B (US.EPA 2003) digestion on the ash was repeated;

2.4.3 The HF digestion analysis.

An HF digestion analysis was done to recover elements (metals) bound into the silica and were not extracted by the EPA 3050B method.

The following HF testing method was used in this project

1. About 1 gram of EPA3050B digested residue (or blank quartz) was accurately weighed into a 35 mL platinum crucible;
2. 2 mL DI water was added to wet the sample;
3. 10 ml HF and10 mL $HClO_4$ were added;

4. The platinum crucible was placed on a boiling water bath then evaporated uncovered till the reaction subsided and the sample solution become clear (additional 5ml HF may be added for SiO_2 blank test);
5. The platinum crucible was cooled slightly and the platinum crucible bottom was dried off;
6. The platinum crucible was carefully transferred onto a low temperature hotplate;
7. It was evaporated until the platinum crucible was fully dry (with no white smoke);
8. Platinum crucible was cooled down then deionized water was used to rinse off the side of platinum crucible;
9. Another 5 mL $HClO_4$ was added;
10. The platinum crucible was placed onto low temperature hot plate then it was evaporated to fully dry (with no white smoke);
11. Platinum crucible was cooled down then the residue was dissolved with 5 mL concentrated HCl;
12. The sample solution in the platinum crucible was accurately transferred into a 50 mL volume flask then topped up with deionized water or AA buffer solution* (refer to ASTM C146 (Baldini et.al, 1996));
13. ICP / AA analysis;

* It was analysed that there is heavy zinc contained in AA buffer solution but no seriously high level of chromium, copper, magnesium, iron and lead detected.

This test is modified from the ASTM (American Society for Testing and Materials) C146 – 94a (Standard Test Methods for Chemical Analysis of Glass Sand) (C.Baldini and et.al 1996) and the UDC (Universal Decimal Classification) 666.123:543.06 (Methods of Chemical analysis of Soda-lime-Alumina and borosilicate glass) (H.R. Li 1994).

The HF reaction first releases the metal from the silica matrix (conventionally shown as an oxide) then the metal is dissolved with HCl.

$$MO\text{-}SiO_2 + 4HF \rightarrow SiF_4\uparrow + 2H_2O\text{-}MO \qquad \text{Equation 2.1}$$

$$H_2O\text{-}MO\ (\Delta) \rightarrow MO + H_2O\uparrow \qquad \text{Equation 2.2}$$

$$MO + 2HCl \rightarrow MCl + H_2O$$ Equation 2.3

2.5 ICP and Atomic Absorption analysis method

1. PERKIN ELMER 3110 Atomic Absorption Spectrometer was used in this research or a Varian Liberty AX Sequential ICP-AES.
2. ASTM E663 – 86 (Re-approved 1991) (Standard practice for flame atomic absorption analysis) (Baldini et.al, 1996) was adopted for sample preparation.
3. Analytical conditions were established following the methods in "Standard Methods for the Examination of Water and Wastewater" (Andrew D. Eaton & Lenore S. Clesceri et al., 1995)
4. Parameters used in ICP and AA analysis see appendix - 1.

2.6 Chemical reagent and its impurity

chemical reagent	
Nitric Acid:	70% HNO_3, Univar, analytical grade, UN No.2031.
Hydrofluoric Acid:	40% HF, BDH AnalaR, U.N. No.1790.
Hydrochloric Acid:	37% HCl, Scharlau, Reagent grade, ACS ISO, AC 0741.
Cupric Oxide:	B.D.H. AnalaR Analytical Reagent, Product No. 10090.
Magnesium Oxide:	B.D.H. AnalaR Analytical Reagent, Product No. 10150.
Lead Oxide:	B.D.H. AnalaR Analytical Reagent, 459614/600601.
Zinc Oxide:	B.D.H. AnalaR analytical Reagent, 671078/501108.
Sodium hydroxide:	Scharlau reagent grade, ACS ISO, SO 0425

Table 2.3 Chemical reagents used in this project

	Chemical reaction impurity						
	Acid-Insoluble matter (%)	Chromium (Cr) (%)	Copper (Cu) (%)	Iron (Fe) (%)	Lead (Pb) (%)	Magnesium (Mg) (%)	Zinc (Zn) (%)
HF	0.005000 Fluorosilicate (SiF6)	0.000020	0.000020	0.000020	0.000005	0.000020	0.000005
HCl	NA	0.000001	0.000001	0.000010	0.000001	0.000005	0.000005
HNO_3	NA	0.000005	0.000002	0.000020	0.000005	0.000020	0.000010
CuO	0.020000%	NA	NA	/	0.050000	NA	NA
PbO	0.010000%	NA	NA	0.001000	0.010000	0.001000	0.003000
MgO	0.100000%	NA	NA	0.001000	0.002500	/	NA
ZnO	NA	NA	NA	NA	0.000500	0.010000	NA
NaOH	NA	NA	<0.0005	<0.0005	<0.0002	<0.002	<0.0005

Date labelled on bottle

Table 2.4 Maxim limits of impurity of chemical reagent

Chapter 3. Results and discussion

In this project, EPA3050B and HF digested specimens were analysed by either AA or ICP. Test confidence interval and standard deviations are given in Figure 3.4-6 and the appendix 7.

The milling times and conditions used represent an evolution in methods as time goes on. Initially the 4 hours milling time used by Bellingham (2006) was adopted but later, some samples were milled for more than 30 hours (in two examples 160 hrs) as reactions were found to continue for well beyond 4 hours.

The whole process including ball milling, EPA3050B and HF digestions is, unfortunately, a very long process and while it would have been desirable to go back and extend some of the earlier milling times or to repeat selected analyses completely so that all samples were milled with the same times and conditions, time constraints meant this was not possible.

These are complex reactions which include some milling jar and milling ball wear, metal oxide reactions with the quartz and with the milling jar and presumably some other reactions with moisture and air. It was found that simple linear regression lines were obviously not appropriate and quadratic curve fitting at times washed out some of the short term features that were observed at 5 minutes and 1 hour milling times. As a result, in this project a 2 point moving average trend line was used for all graphs.

3.1 Copper oxide milled with silica

Since copper is one of the metal markers for anthropogenic pollution (the others are commonly lead and zinc), and copper is easy to analyse by AA and ICP, CuO was initially selected in this research to mill together with SiO_2.

3.1.1 CuO and quartz in 500 mL steel jar – EPA 3050B digestion

1% of CuO (0.5 grams CuO in 49.5 grams silica) was milled with SiO_2 in a steel jar. 2 grams of sample was taken at intervals of 5 minutes, 1 hour, 2 hours, 3 hours and 4 hours respectively. 1 gram of each milled powder was digested by EPA3050B.

The results are shown in Figure 3.1-1 which is detected copper vs. total reactant (copper oxide with silica) in ppm.

A comparison of CuO milled with quartz in the steel and zirconia jars (Figure 3.1-3) are presented in Figure 3.1-1 as absolute concentrations in ppm and as a percentage of the original concentration Figure 3.1-2.

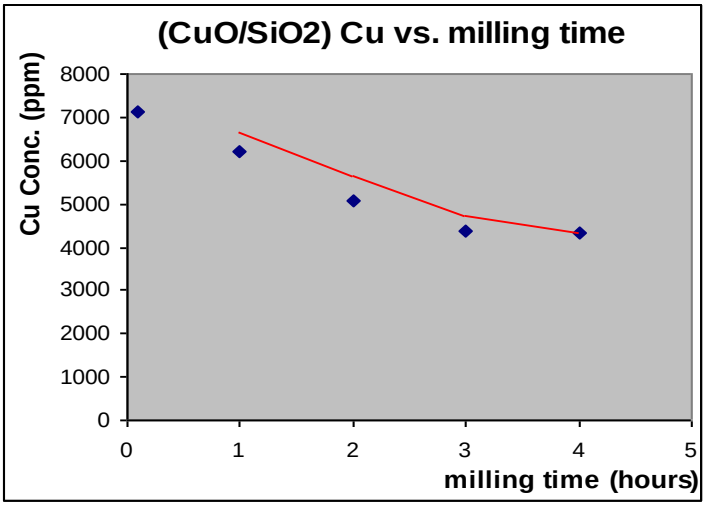

Figure 3.1-1 Detected copper Conc. (ppm) after 4 hours CuO milled with quartz and digested by EPA3050B method.

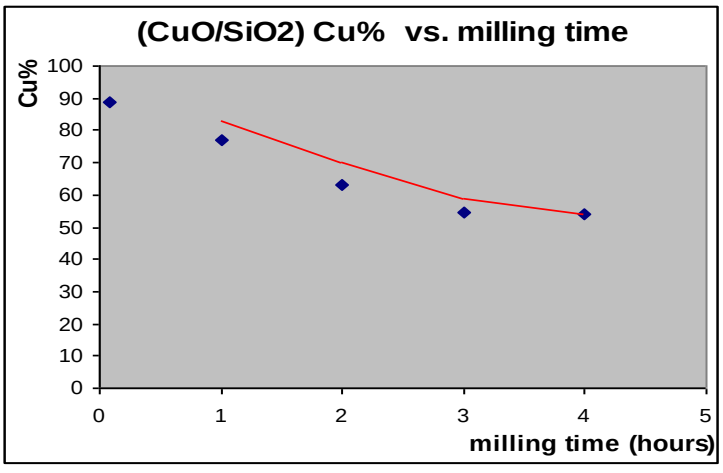

Figure 3.1-2 Detected copper Conc. (percentage) after 4 hours CuO milled with quartz and digested by EPA3050B method.
* This diagram only used as a comparison with Figure 3.1-3

3.1.2 CuO and quartz in zirconia jar – EPA 3050B digestion and HF digestion of the residue

Murty and Ranganathan (1998) reported in some cases iron, worn off from the steel milling jar and milling balls, could be contributing to the reaction. It was obvious in these experiments that the iron and other elements from the balls and milling jar worn off and become a part of the milling reaction. A simple test with a magnetic showed that all samples milled in steel jars with steel balls contained some ferromagnetic material.

In order to clarify the relationship between reactants and the material of the milling jar (chrome steel) and milling balls (mild steel), zirconia milling jar and zirconia milling balls were used with the same milling machine and same milling conditions (milling velocity, milling time, milling matrix) except ball to weight ratio changed from steel milling balls of 5:1 to zirconia milling balls of 10:1 (Because the size of zirconia milling jar is only 10% that of steel jar, the sample size was reduced to 10% compare with the volume used in chromium steel milling jar).

Thus the following procedure was used: 1% CuO (0.05 grams of CuO in 4.95 grams silica) was milled with SiO_2 in zirconia jar: a 2g sample (1g for EPA 3050B digestion and 1g for retention) was taken after 5 minutes milling. After 1 hour milling, the whole sample (about 3 grams) was removed (since the sample size is not enough to do another time sampling), the milling jar was then reloaded with another 5 gram (1% CuO and quartz) specimen. A 2 gram sample was taken after being milled 2 hours; the whole specimen (about 3 grams) was removed after milling for 3 hours. Again, the milling jar was reloaded with another 5 grams (1% CuO and quartz) specimen and after 4 hours of milling, the whole specimen (about 5 grams) was removed. Then 1 gram of each sample from each sampling time interval was taken and digested using the EPA3050B method.

Since there was more than one time of CuO and quartz input during the process, results shown in Figure 3.1-3 are expressed as a percentage of detectable copper vs. copper input. (It is impossible to compare the concentration at different sampling point in ppm in case of the input concentration was different).

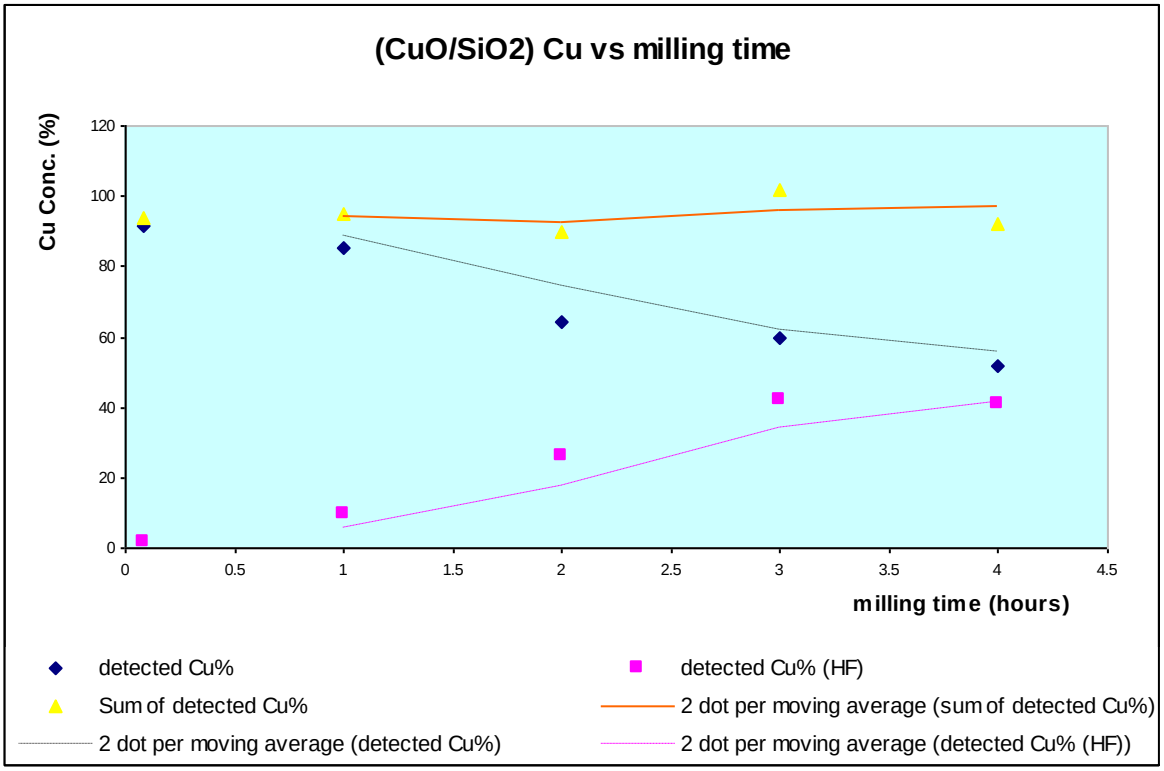

Figure 3.1-3 Detected copper Conc. (percentage) After 4 hours milling CuO with quartz (in zirconia jar); including EPA3050B digestion and HF digestion of the residue.

3.1.3 Summary and comment

Summary:

It can be seen from Figure 3.1-1 and 3.1-2 (milled in a steel jar) after EPA3050B digestion that: the detectable copper concentration significantly dropped.

The experiment where quartz and CuO were milled in a zirconia jar is a very important result because it shows the metal(s) from the jar are not significantly involved in the process that is trapping the copper and preventing its extraction by the EPA3050B method (US.EPA, 2003). EPA3050B extractable copper results in Figure 3.1-3 showed a very similar behaviour to the same experiment done in the larger steel jar (compare Figure 3.1-2).

Likewise, it can be seen from Figure 3.1-3 after the HF digestion of the residue that: most of the copper which was unable to be dissolved by EPA3050B method (US.EPA, 2003) could be released by HF digestion of the residue and the detectable concentration continuously increase (figure 3.1-3).

In the same diagram (Figure 3.1-3), it can also be seen that the sum of copper concentration after EPA3050B digestion and the residue HF digestion maintained in a constancy level which is nearly 90% of the initial input.

Comment:
It can be seen from Figures 3.1-1, 3.1-2 and 3.1-3 that four hours milling time is not enough to bring the milling to a steady state. As noted above, a comparison of the results from the steel jar and zirconia jar showed very similar behaviour, this indicated that the milling equipment does not affect the milling result. It can be seen from Figure 3.1-2 and 3.1-3 that the detected copper concentration of 5 minute samples by EPA3050B digestion and the sum of the detected copper concentration is around 90%.

3.2 Magnesium oxide milled with silica

Based on previous work done by Bellingham, the original work on copper only used a 4 hour milling time. The results showed that the reaction had not reached a steady state, so in this experiment the milling time was doubled (eight hours). It was expected that the milling result should approach the steady state. It was also originally thought that the milling process was forming mineral-like structures which could be identified by infrared spectroscopy or x-ray diffraction. The magnesium silicate minerals are well characterised and it was expected that these experiments would show some evidence of mineral formation.

In this experiment, about 1% MgO (0.5 grams of MgO in 49.5 grams silica) was milled with SiO_2 in the steel jar. Two gram samples were taken at 5 minutes, 1 hour, 2 hours, 3 hours, 4 hours, 5 hours, 6 hours and 8 hours respectively. After milling, 1 gram of milled powder from each sample was digested by EPA3050B.

Results are shown in Figure 3.2 and calculated in ppm which is detectable magnesium vs. total reactant (magnesium oxide with quartz).

3.2.1 MgO and quartz - EPA3050B digestion and HF digestion of the residue

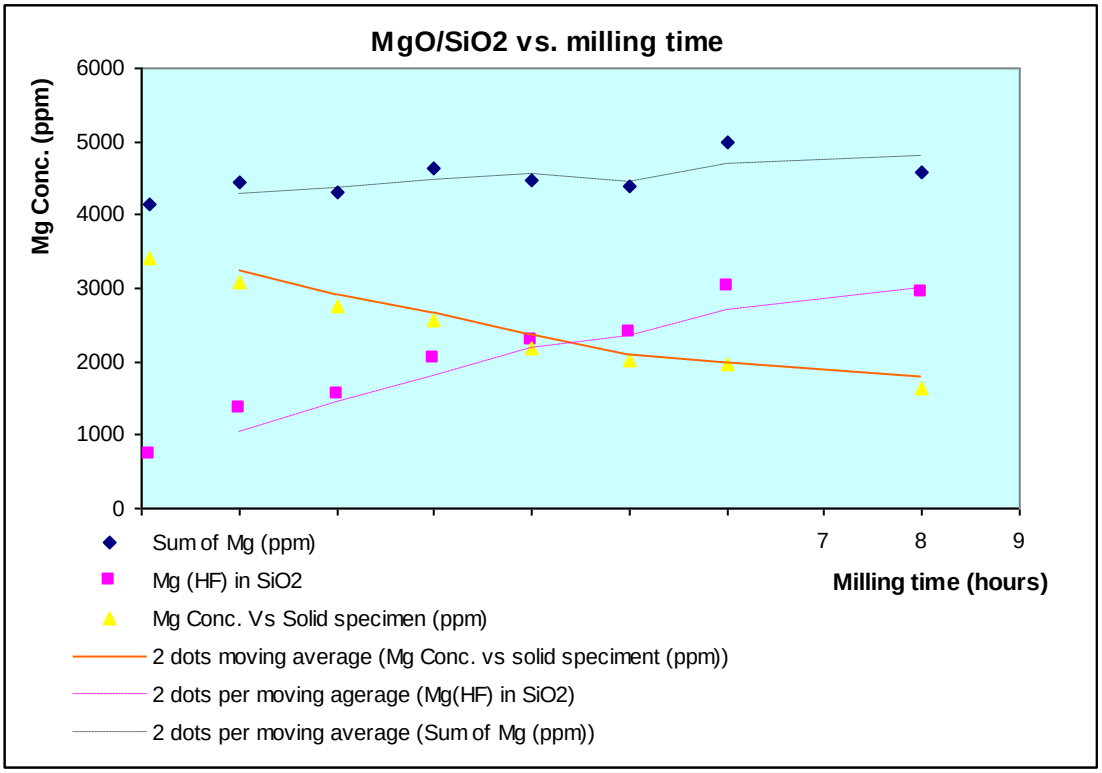

Figure 3.2 Detected magnesium conc. (calculated in ppm) 8 hours milling MgO with quartz (in steel jar); digested by EPA3050B method.

3.2.2 Summary and comment

Summary:

From the EPA3050B digestion curve, it was found that the detected magnesium concentration continued to decline. Meantime it was found from the residue HF digestion curve that the detected magnesium concentration in quartz continues increasing. However the sum of the two curves is about 4500 ppm level, which is only about a 75% recovery.

Comment:

MgO and quartz (Figure 3.2-1) is similar to the CuO and quartz milling system (Figure 3.1-1 and 3.1-3), and data from MgO and quartz provided more evidence that after metal oxides are milled with quartz, metal will be synthesised with quartz. It is estimated that the similarly as magnesium other alkaline earth silicates could be mechanochemically formed with silica.

Even though in this experiment 8 hours milling did not bring the MgO and quartz milling system to a stable state, the reaction is apparently approaching a stable state.

3.3 Lead oxide milled with silica

Even after eight hours milling, the MgO milled with quartz experiment showed that the reaction still has not reached the steady state. The following experiment was designed to extend the milling time to thirty hours. It is expected that the reaction could reach or be close to a steady state after 30 hours milling.

Lead, as one of the heavy metals in the environment, was used in the following experiment to see if the environmental pollutant could be immobilised in milled quartz. As well as investigating the sequestering of lead, this experiment was intended to investigate the levels of iron and chromium that wear off the steel milling jar and milling balls with prolonged milling.

It was expected that: after thirty hours milling, the reaction could reach a stable state, and the sum of detectable lead concentration from both digestion methods should be constant for all samples. Certainly iron and chromium contamination should be detectable, but the levels and rate of ball/jar wear were uncertain,

In this experiment, 1% PbO (0.5 gram PbO in 49.5 gram silica) was milled with the quartz in a steel milling jar. Two gram samples were taken at 5 minutes, 1 hour, 2 , 4 , 6 , 8 , 12 , 16 , 20 and 30 hours respectively. After milling, 1 gram of milled powder from each sample was digested by EPA3050B.

The results are shown in Figure 3.3-1, 3.3-2, 3.3-3 and 3.3-4 and calculated in ppm which is detected metal vs. total reactant (lead oxide with silica).

3.3.1 PbO and quartz - EPA3050B digestion and HF digestion of the residue

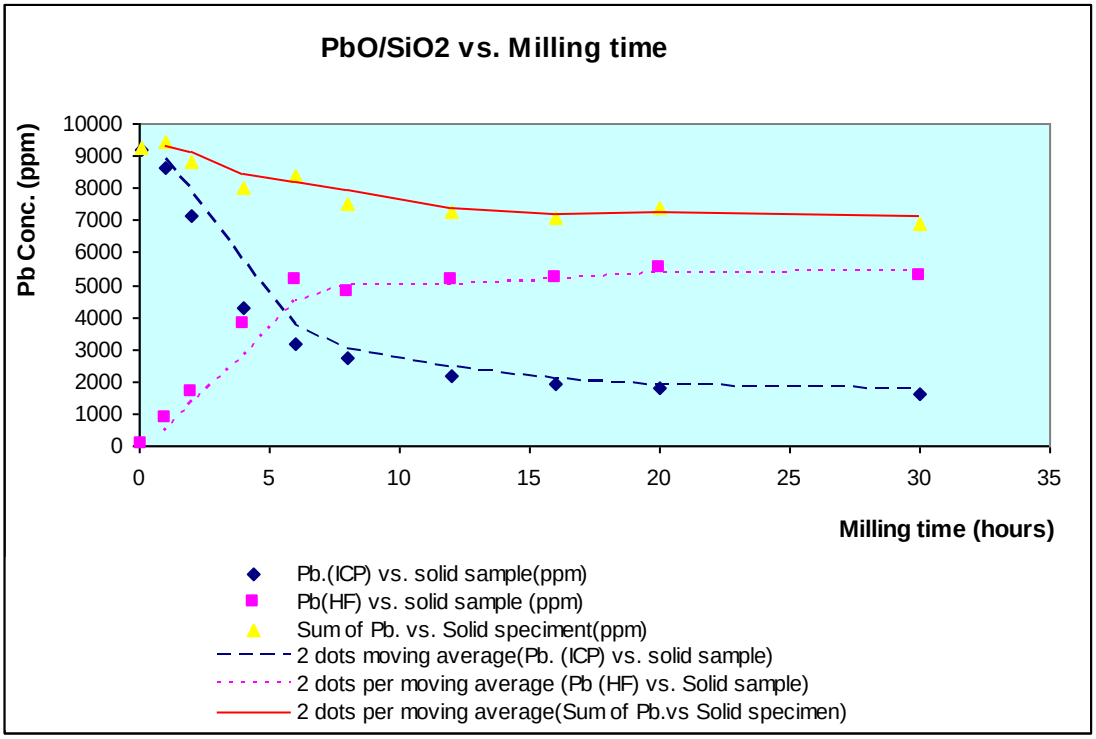

Figure 3.3-1 Detected lead conc. (calculated in ppm) in the (PbO and quartz) milling system, including EPA3050B and HF digestion.

Summary:

It was found from the EPA3050B digestion curve in Figure 3.3-1 that with up to thirty hours milling, lead concentration in samples digested by EPA3050B formed a decay curve and the trend line dropped significantly during the first 6 milling hours. After 8 milling hours the slope of the curve flattens noticeably.

As was found for earlier copper and magnesium experiments, the sequestered lead from the HF digestion of the residue is increasing while the EPA3050B extractable lead decreases. It is interesting to note that the lead concentration from the HF digestion increased sharply in the first 6 hours then levelled off. This is mirrored to a certain extent by the drop in the EPA3050B extractable lead.

Comment:

The results for PbO milled with quartz (Figure 3.3-1) show a similar pattern to the CuO and quartz results (Figure 3.1-1) for the first 4 hours, and are also similar to the MgO and quartz results (Figure 3.2-1) in the first 8 hours. Both of the EPA3050B

digestion curves and HF digestion of the residue curves in opposite directions, provided further evidence again that the undetected lead by EPA3050B method was incorporated with the silica structure (or it could be said to be 'sheltered' by SiO_2). It is thought that, the same as lead, other metals may be mechanochemically sequestered with quartz.

That the curve changed sharply during the first 8 hour of milling is interesting. It shows that the initial reaction between lead and silica is at a fairly high rate, but between 8 and 10 hours the process seems to undergo some change. While some sequestering is still in progress there is a suggestion that some other mechanism is becoming involved. See section 3.7, section 3.8 and the discussion for more thoughts on this process.

It was expected the sum of recovered lead (digested by EPA3050B together with that released by HF digestion of the residue) should be a constant line close to theoretical (which is a straight line parallel to X axial), but obviously in the diagram, the sum of recovered lead in the 5 minutes sample is above 9000 ppm, which is very close to the input. However the curve for total recovered lead dropped after that. This means that, in the same way there was less than 100% recovery, as for the CuO and MgO experiments, with some of lead also appearing to be "lost" during milling and is not recovered by EPA3050B and HF digestion of the residue at this stage.

While care was taken in the manipulation of the samples there was a consistent small loss in total recovery. The following reasons are thought to be involved to a greater or lesser degree:

1. Lead contamination on the surface of milling jar and balls (Figure 3.4-3) during the milling process. (It will be discussed in section 3.4.3)
2. Residual iron and chromium from the milling jar and balls could lead to an error (discussed in section 3.3.2).
3. Although the residue was scratched off from the filter paper for the HF test, the filter paper did not ash in this test, this may result in some of the lead together with quartz powder being adsorbed onto the filter paper, (compare with section 3.4 and Figure 3.4-5) and hence the total detected lead was reduced.

3.3.2 Milling jar and balls wear

When steel balls and jar are used in mechanochemical processing there is obvious ball and jar wear. The ball wear in dry milling is entirely due to abrasion and erosion (Tkacova & Stevulova et al., 1995). If the material of the milling jar is different from that of the powder, material dislodged and incorporated into the powder can potentially alter the chemistry of the powder or contaminate the powder with the milling jar material (Suryanarayana, 2001). Indeed the samples always have some ferromagnetic iron in them that can be seen when a magnet is held close to a sample. Ball-powder-ball collision in a rotating or vibrating jar is considered to be the main source of iron contamination (El-Eskandarany & Aoki et al., 1990).

It is reported that oxides can be formed when milling metals in the presence of atmospheric oxygen. "The rate of oxidation passes through a maximum, depending on the duration of milling" (Boldyrev & Avvakumov, 1971).
The following equation describes the oxidation rate of metal before it reaches the maximum.

$$LnV = KT + C \qquad \text{Equation 3.1}$$

V is the rate of oxidation, K and C is constants, (Boldyrev and Avvakumov 1971)

In this study, no attempt was made to identify the actual form of the wear material. Information from Retsch GmbH (2006) states the milling jar is chrome steel -- 12.000% chromium and 84.890% iron (appendix – 4). As a result, the chromium and iron concentrations were also measured for selected experiments.

3.3.2.1 Chromium contamination

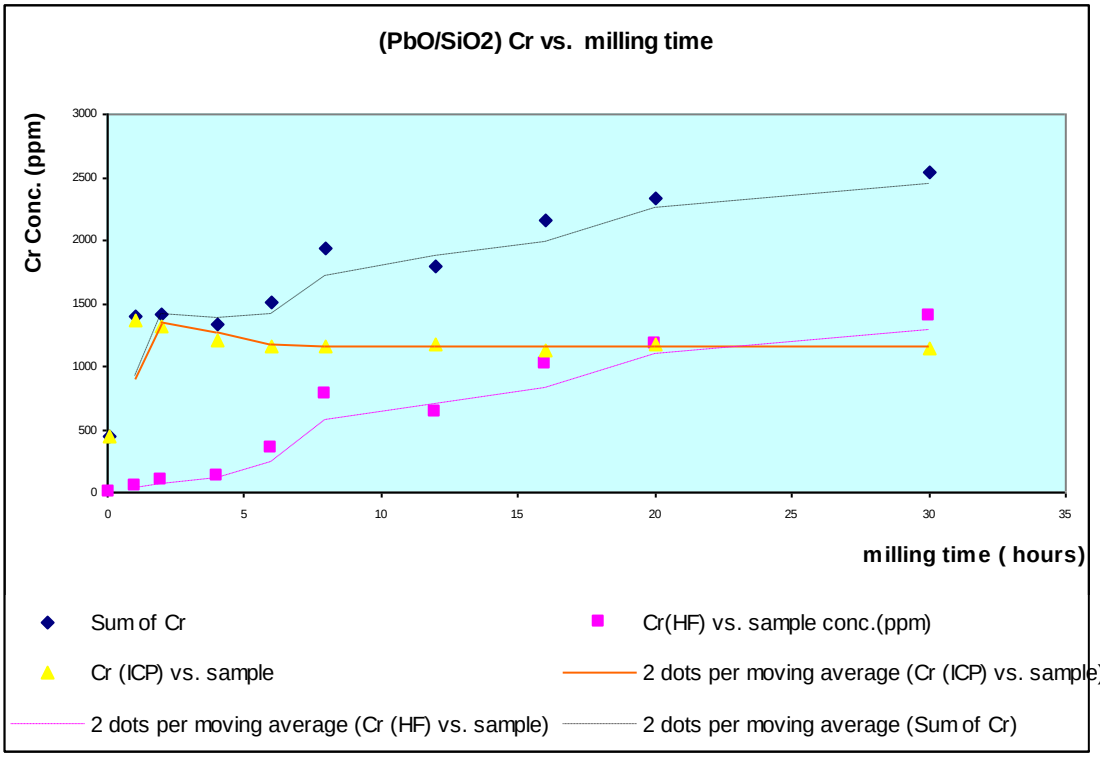

Figure 3.3-2 Cr contamination in the (PbO and quartz) milling system, including EPA3050B and HF digestion.

Summary:

From this diagram it can be seen that the chromium concentration, which could be digested with the EPA3050B digestion method, is almost constant except for a peak in the first 1 hour sample, and the chromium concentration, which could be released with HF digestion of the residue increased proportional to the milling time. Same as the residue HF digestion curve, the sum of chromium contamination (wear off) increased proportional to the milling time and reached 2500 ppm level (0.25% wt./wt. Cr vs. PbO and quartz) in the end of milling.

Comment:

Chromium contamination must represent the wear from the milling jar. Iron can come from both the balls and the jar. The chrome steel is a much harder and tougher material than the mild steel balls that were used; as a result ball wear will not be the same as jar wear. This will be discussed in more detail later.

Compared with the concentration increase being proportional to milling time by HF digestion of the residue, there is almost no changing of the detected chromium by the EPA3050B method.

The small peak that appeared in the initial 3 hours by EPA3050B digestion may indicate that the initial chromium lost from the jar while the quartz particles are larger (and more abrasive) has not yet reacted with the silica. After about 1 hour of milling, the sequestering process begins to become important. Again, there is some evidence for this in the changes of particle sizes during milling (Figure 3.7-1, 3.7-2 and 3.7-3). A similar peak is also seen during the analysis of the chromium (figure 3.4-4) and lead (Figure 3.4-3) in the sample of zinc oxide milled with quartz.

3.3.2.2 Iron contamination

The analysis of iron contamination gave the following:

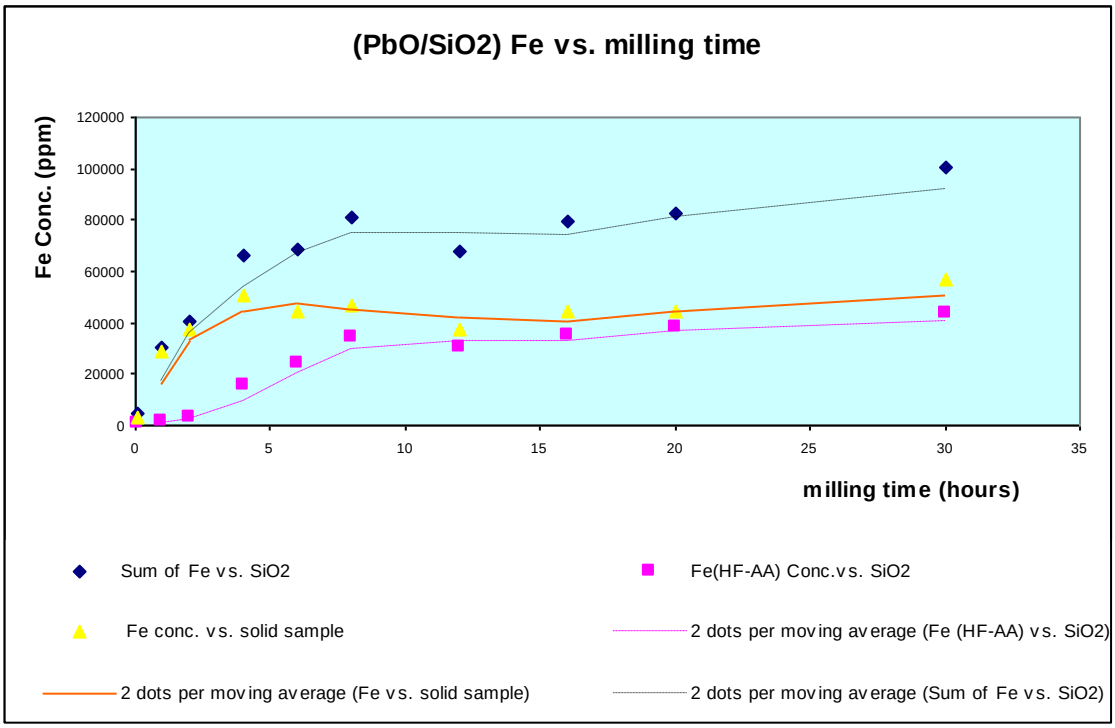

Figure 3.3-3 Fe contamination in the (PbO and quartz) milling system, including EPA3050B and HF digestion.

Summary:
It can be seen from the figure 3.3-3 that there is a peak in the 4 hour sample in the EPA3050B digestion curve and after 8 hours milling the iron levels begin to level off. Again there is the suggestion that particle size has an effect on wear rates and possibly on the sequestering mechanism.

From this diagram it can also be seen that after 30 hours, the chromium contamination level is about 2500 ppm (0.25%) and the iron contamination level could reach as high as 100,000 ppm (10% w/w).

Comment:
The iron levels do not increase as a simple function of milling time; the contamination shown in Figure 3.3-3 represented the iron wear off from both milling jar and balls (compare with chromium contamination from milling jar only which has been discussed earlier) and both of iron concentration curves (EPA3050B and HF digestion) increase indicated that the rate of iron wear is higher than the rate of sequestering.

As noted above, for chromium (Figure 3.3-2), the peak appeared in the initial 3 hours in the EPA3050B digestion, indicating the significant particle size reduction caused the iron wearing off again. It is suspected that not only the size and shape of quartz but the material of milling balls and milling jar play an important role during the worn off (contamination) of iron and chromium as well.

It has been noticed that starting from 5 minutes to 30 hours milling, in the EPA3050B digested residue, colour changed from white to deep grey (the colour become darker and darker). The colour change may relate to the Fe contamination. This type of colour change happened in all other oxides milled with quartz in steel jar as well.

If the worn off metal is an additional metal input, it must be allowed for quantitatively (it is diluting the sample) and considered as a potential reactant in the mechanochemical process.

3.3.2.3 Comparison of milling results allowing for iron contamination

In the following diagram, allowances are made for the progressively increasing proportion of iron in the samples.

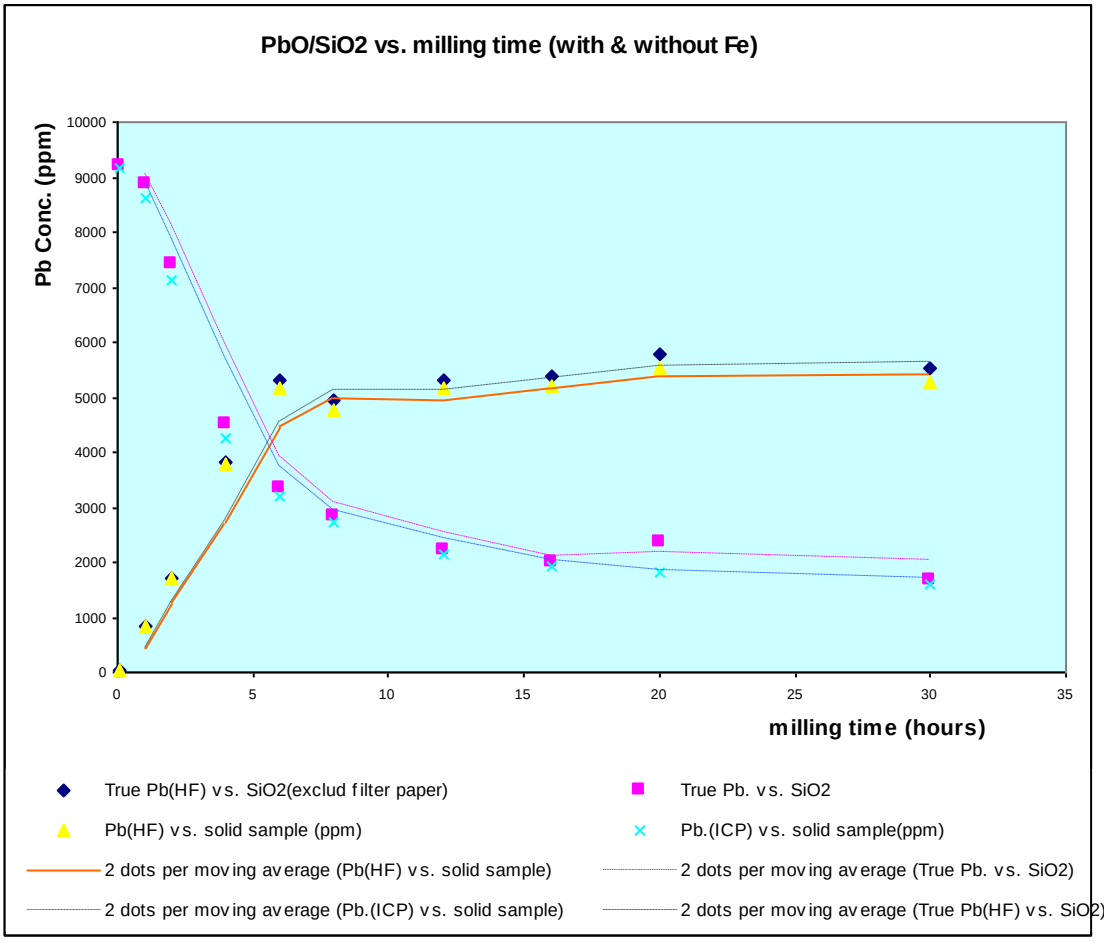

Figure 3.3-4 Detected lead conc. After 30 hours milling PbO with quartz; including EPA3050B and HF digestion. (comparison of the Pb Conc. with vs. without Fe contamination)

* True Pb vs. SiO_2 indicates without Fe contamination.

Summary:

From Figure 3.3-4 it can be seen that although making allowance for the iron having some effect on the absolute levels, when compared to Figure 3.3-1, the relative shape of the curve is largely unchanged.

Comment:

Because of the iron contamination the detected lead concentration had been diluted a little. This may be the reason for the sum of detected lead concentration being reduced by the end of the process (refer to figure 3.3-1)

3.4 Zinc oxide milled with silica

As there was some question on how efficient the EPA3050B digestion was, for the ZnO and quartz samples, a sequential set of further EPA3050B digestions was done. Because the structure of the EPA3050B digested residue and its thermo-stability was not clearly understood, in order to minimize the structure and thermo-stability change at 650^{o}C and half an hour ashing treatment -- which could affect the digestion result, after the first digestion, the EPA3050B digestion residue was scratched off from filter paper as thoroughly as possible. Meantime in order to identify the quantity of residue adsorbed onto the filter paper, the filter paper was ignited and ashed in a furnace at 650^{o}C for 30 minutes. The ashed residue was then combined with un-ashed (scratched) residue. (There was roughly 10% of residue adsorbed onto the filter paper, see Figure 3.4-5.) Finally the combined residue was collected and digested a second time and third time using the EPA3050B method. It is expected the first EPA3050B digestion was sufficient, so the second and third digestions using the EPA3050B method digestible zinc remaining in the residue (digested powder) should be minimal.

Since in the last experiment, the sum of lead concentration was not in constant, it was suspected that some of the lead reacted with the milling jar and milling balls. The following experiment was designed to detect any lead that had become "stuck" to the jar and balls. A new experiment reacting zinc oxide with quartz was done after the lead work and the levels of lead and zinc were determined.

In this experiment, 1% ZnO (0.5 grams ZnO in 49.5 grams silica) was milled with quartz using the 500 mL steel jar and balls. Two gram samples were taken at 5 minutes, 1 hour, 2 hours, 3 hours, 5 hours, 7 hours, 9 hours, 12 hours, 16 hours, 20 hours and 30 hours. After milling, 1 gram of milled powder from each sample was digested using the EPA3050B method followed by an HF extraction of the residues. The result is calculated in ppm which is detected Zn vs. total reactant (zinc oxides with silica).

Note: the second and third extractions are included in this figure but are discussed in more detail in section 3.4.2.

3.4.1 ZnO and quartz – EPA 3050B digestion and HF digestion of the residue

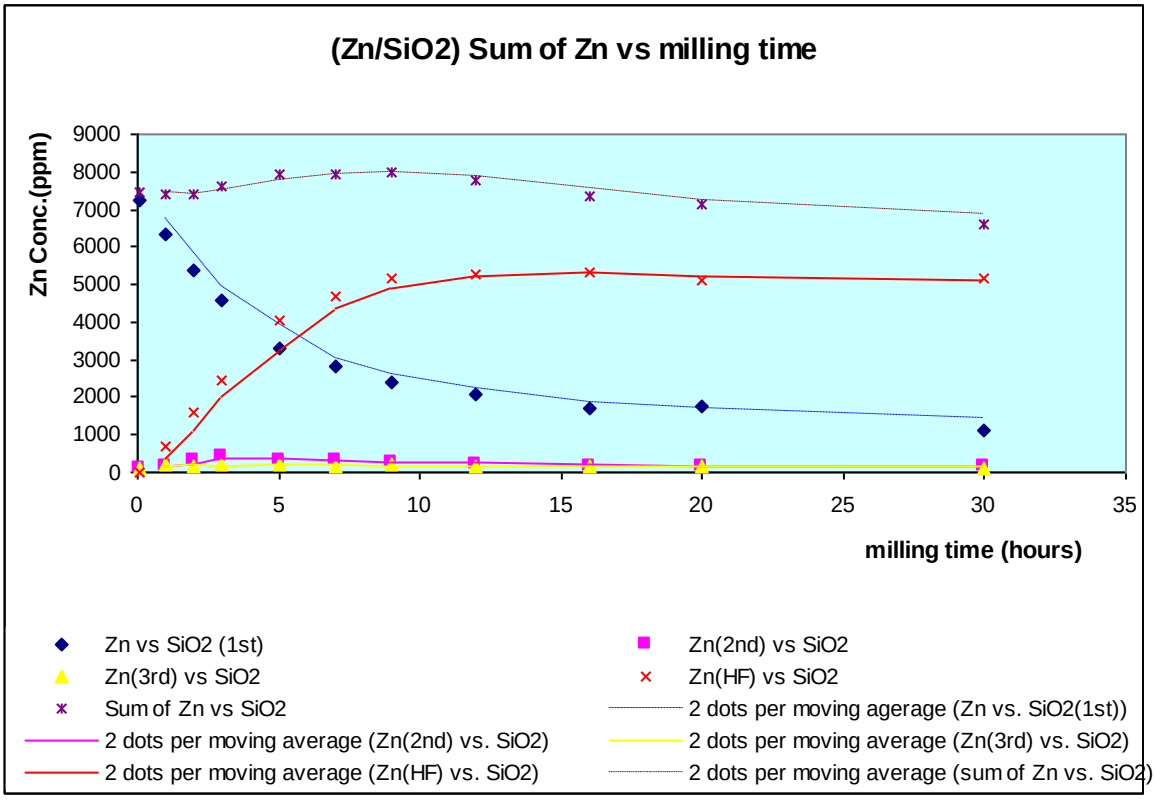

Figure 3.4-1 Detected zinc Conc. (ppm) After 30 hours milling ZnO with quartz; including 3 times EPA3050B and HF digestion.

Summary:

Figure 3.4-1 showing the EPA3050B digestion curve, it can be seen that there is an obvious significant difference between the first EPA3050B digestion and the second and third EPA3050B digestions. The second and third digestion results in Figure 3.4-1 are nearly linear in this scale of diagram being fairly close to the base (zero) line and nearly covering each other.

From Figure 3.4-1, showing the HF digestion of the residue curve, it can be seen that the detectable zinc concentration is increasing in the opposite direction to the EPA3050B curve. It increased sharply in the initial 7 hours, then levelled out.

Comment:

The tendency of the whole ZnO and quartz EPA3050B digestion curve agrees with the previous work. The second and third EPA3050B digestion results compared to the first EPA3050B digestion indicate the first digestion by EPA3050B is able to extract

at least 95% of the extractable metal. Clearly then metals are being sequestered in the ball milling process and that to get a proper result for total metal concentrations, exhaustive HF digestion is necessary.

The curve of the sum of zinc (detected EPA3050B digestion together with HF digestion of the residue) shows about 7500 ppm recovered, which compares well with the approximately 8000 ppm zinc input, hence, the recovery rate is over 90%. It is suspected that the un-recovered zinc reacted with the milling balls and milling jar.

3.4.2 Zinc concentration change during second and third EPA3050B digestion

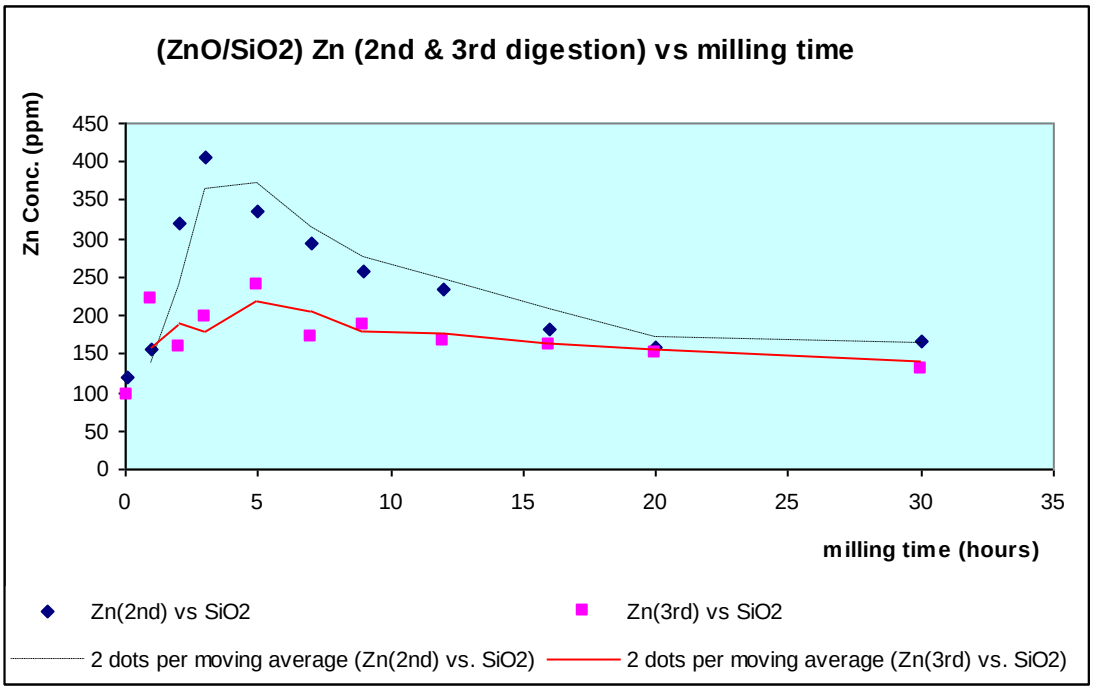

Figure 3.4-2 Detected zinc conc. (calculated in ppm) After 30 hours milling ZnO with quartz ; including 2nd and 3rd times EPA3050B digestion

Summary:

Figure 3.4-2 is the diagram which enlarge the curves of second and third digestion of ZnO and quartz by EPA3050B (Figure 3.4-1). It can be seen from Figure 3.4-2 that there is a peak of zinc concentration change in the initial 9 hours in the second EPA3050B digestion curve, the peak reaching its highest at around the 4 hour point. The highest point of this peak (zinc concentration) appeared at around 400 ppm level (compare to nearly 8000 ppm zinc input, and around 2000 ppm in the 30 hours of first

EPA3050B digestion). The peak appeared in the second EPA3050B digestion curve and was exhausted in the third EPA3050B digestion.

Comment:
Once again the curves show an initial peak in the extractable element. It is suspected that because of the high concentration of ZnO, the mechanochemical reaction during first 10 hours period was fairly strong, but the product structure is relatively weak. (it may only reach a meta-stable state), and this kind of meta-stable structure leading the zinc concentration curve reached a peak during this time period in the second and third EPA3050B digestion. However the peak disappeared after 15 hours milling in the second EPA3050B digestion, indicating that come with the continued energy input, the product structure was getting more stable (part of product transfer from meta-stable state to stable state).

The type of metastable state and the mechanochemical reaction during this period could be understood as the evidence of brittle material such as quartz breaking down in the initial milling time in a small area or into a small particle and then deforming itself plastically. This probably could be explained with "particles size – plastic behaviour" concept which has been discussed in section 1.2.4.4.

3.4.3 Lead contamination

In the last experiment, the sum of lead concentration which did not reach the balance (Figure 3.3-1) was suspected to have reacted with the milling jar and milling balls, so as noted previously, the residual lead levels were also analysed.

It should be emphasised that initially there is no input of lead in the ZnO and quartz milling system. The main possible source of lead could be from the previous milling (PbO milled with SiO_2).

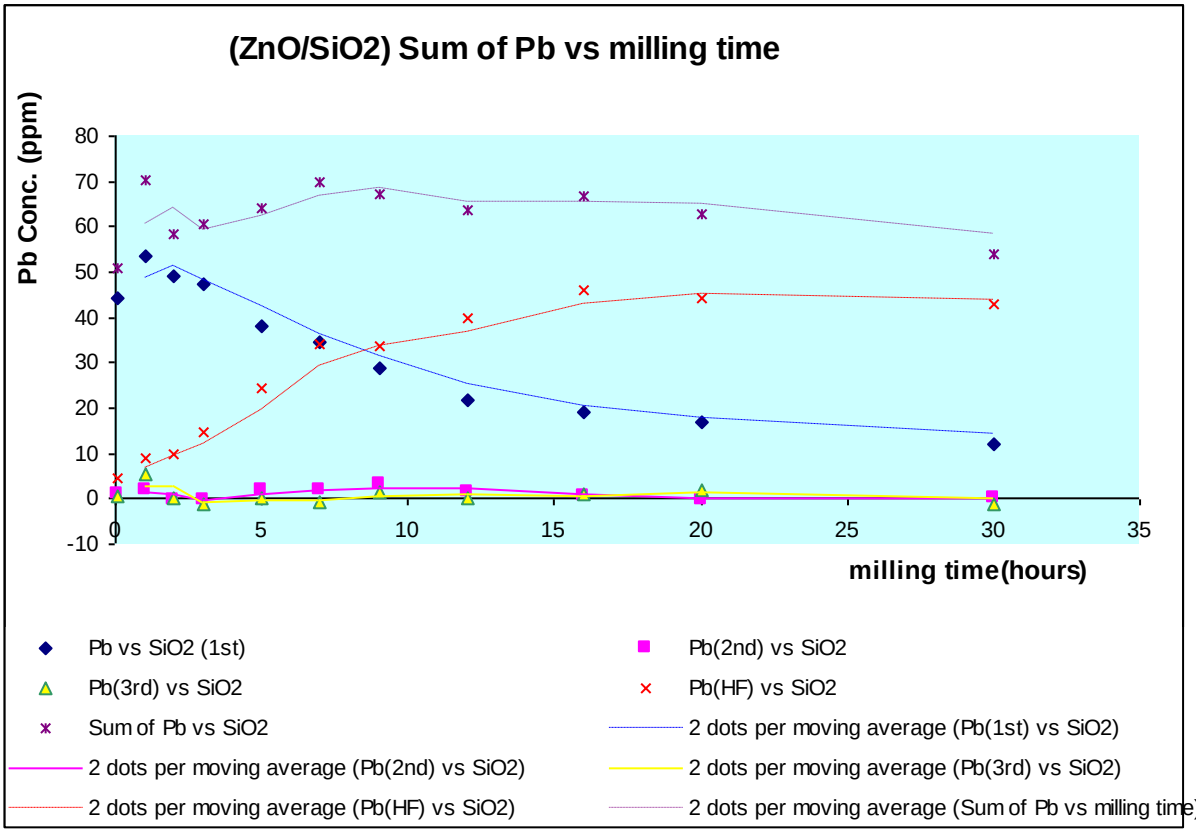

Figure 3.4-3 Sum of Pb contamination in (ZnO and quartz) milling system, including 3 EPA3050B digestion and HF digestion of the residue.

Summary:

From the EPA3050B digestion curve in Figure 3.4-3, it can be seen that in the 80 ppm scale diagram, the maximum level (sum) of lead is less then 70 ppm (compared with the 9000 ppm input into the PbO and quartz milling system in the last experiment).

The lead concentration declined in the first EPA3050B digestion and is very similar to the results in Figure 3.3-1 except for a small peak in the 1 hour sample. But the second and third time EPA3050B digestion result is nearly constant and very close to zero.

From the above diagram – the HF digestion of the residue curve, it can be seen that with the milling time increasing, the detected lead concentration tended to increase in the opposite direction to the first time EPA3050B digestion curve (it gets flatter after the 16 hour point).

Comment:
The pattern of lead contamination in both digestion curves of EPA3050B and HF are similar with Zn and quartz (Figure 3.4-1) and PbO and quartz (Figure 3.3-1). The decline in lead concentration in the first EPA3050B digestion indicated that the quantity of lead in the ZnO and quartz milling system is fixed and the quantity of lead approached exhaustion. This is the evidence that there is no other continued source of lead input into the ZnO and quartz milling system. The second and third time EPA3050B digestions in the lead contamination diagram provided further evidence that the first time EPA3050B digestion is sufficient.

Since there is no lead input, it is recognized that the only contamination source of an average of 65 ppm (varies from time to time) in the ZnO and quartz milling system came from contamination of the last milling experiment (PbO and quartz milling system). That means during last experiment while lead reacted with SiO_2, lead also reacted with the milling balls and milling jar and this contamination is not easily water or brush removable. Those lead remaining on the milling jar and balls has been worn off, together with iron, and become the contaminant in this experiment. This is probably one of the explanations for the sum of Pb concentrations decline with milling time in the PbO and quartz milling system.

In the 1 hour sample, the detected EPA3050B digested lead reached the highest point indicating that, compared with the 5 minutes sampling point and the 2 hour sampling point, most of lead had worn off by the 1 hour sampling point. It is worth noting though that even after 30 hours milling there is still some 15 ppm of lead detectable from the completely separate previous experiment. This would be significant if the sample was to be used for an environmental assessment.

Compared to about 2000 ppm of “lost” lead from the previous experiment, this is actually a fairly trivial recovery. In this experiment there was only less than 70 ppm of lead recovered. The other un-recovered lead has been discussed in section 3.3.1.

3.4.4 Chromium contamination

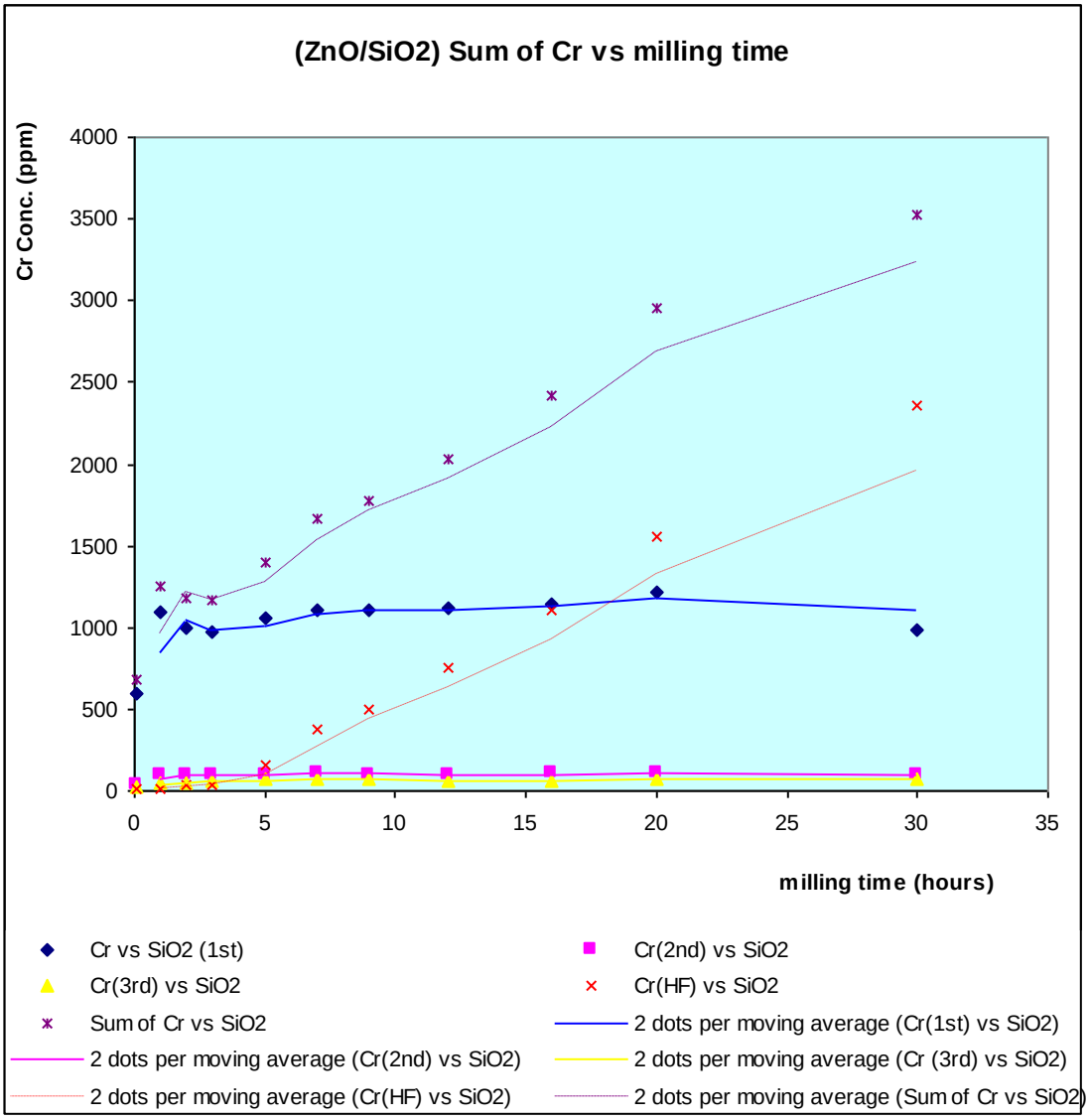

Figure 3.4-4 Sum of Cr contamination in (ZnO and quartz) milling system, including 3 times EPA3050B and HF digestion.

Summary:

It can be seen from Figure 3.4-4 that the detected chromium concentration results are similar to those for the PbO and quartz system (Figure 3.3-2) both in levels of chromium and the shape of the plot.

The chromium concentration curve, which was digested with first EPA3050B digestion, is almost constant except for a small peak in the 1 hour sample point (as was seen in Figure 3.3-2 and others). While the second and third EPA3050B digestion curves are almost constant and covered each other, close the base line.

It also can be seen from this diagram that the concentration of chromium that could be released with the HF digestion of the residue, increased significantly, and this resulted in the sum of chromium concentration (from mill wear) increasing significantly.

Comment:
Since chromium contamination in the ZnO and quartz milling system agreed with the chromium contamination in the PbO and quartz milling system, the iron contamination in the ZnO and quartz milling system also agreed with the iron contamination in the PbO and quartz experiments.

The peak appearing at the 1 hour sampling time in the first time EPA3050B digestion curve of chromium in the ZnO and quartz milling system (Figure 3.4-4) agrees with the peak that appears in the EPA3050B digestion curve of chromium in the PbO and quartz milling system (Figure 3.3-2) and agrees with the peak appeared in the EPA3050B digestion curve of iron contamination in the PbO and quartz milling system (Figure 3.3-3). Again, this is related to the results of milled particles size measurement (Figure 3.7-1 to Figure 3.7-7) which show that the particles size significantly reduces in the initial milling period and is consistent with a change in the sequestering process.

3.4.5 Thermo-stability

As mentioned in 3.3.2.2, after the EPA3050B digestion, residue colour changed from pale white to deep grey. But in this experiment, it was noticed that after ashing, the colour of residue adsorbed on the filter papers changed from pale white to deep brown from 5 minutes to 30 hours respectively (see Figure 3.4-5).

It is assumed that the high concentration of iron (about 10%) was further oxidized during ashing and resulted in this colour change. If there had been a mechanochemically induced reaction to form an iron-quartz structure it may have been thermally unstable during ashing (650^{o}C for 30 minutes). If this is true then other metal-quartz structures may be thermally unstable as well. Because of the limitation of time, no further research was carried out in this area in this project.

Figure 3.4-5 the comparison of residue of second EPA3050B digestion (grey colour) and the ashed residue of second EPA3050B digestion (brown colour) in the 2 hours sampling time vs. the 30 hours sampling time.

3.4.6 Test confidence interval

The test confidence interval and standard deviation of ZnO and quartz for the first time EPA3050B digestion has been checked and calculated, (see Figure 3.4-6 and appendix - 7 for details).

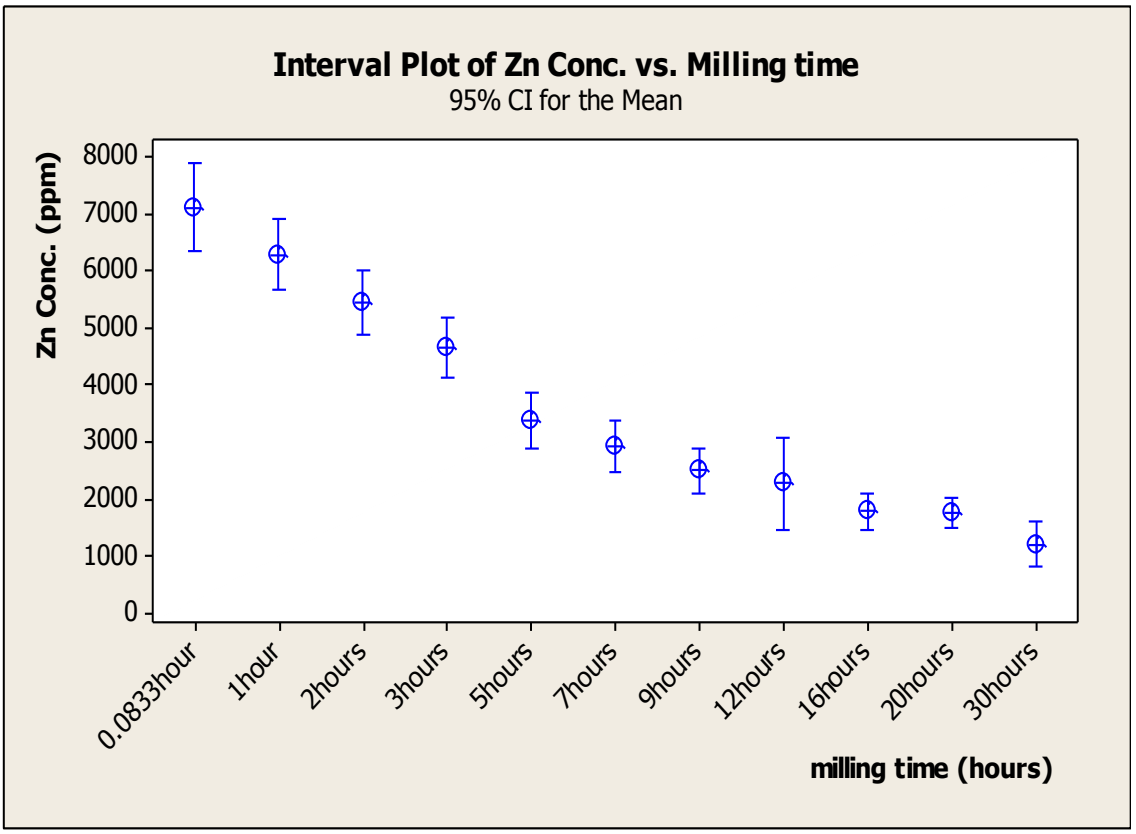

Figure 3.4-6 interval plot of detected Zn by first EPA3050B digestion in ZnO and quartz milling system

3.5 Sodium hydroxide milled with silica

All above experiments provided evidence that after processing with high energy ball milling, copper, zinc, iron, chromium (transition metals), magnesium (alkaline earth metals) and lead oxides were sequestered in some way by the quartz.

Initially it had been assumed that these metal oxides were forming insoluble metal silicates but Jiang and Zhou et. al (1996) reported that up to 21 hours milling, there was no reaction found between α-Fe_2O_3 and SiO_2, by milling hematite (α-Fe_2O_3) with silica (SiO_2) except the size reduction. Only after 51 hours milling were iron-rich

spinels and iron amorphous silica produced, combined with Fe(II) atoms in its structure. Later these authors reported again that a two-phase system of Fe-rich spinel(s) and a heterogeneous Fe(II)-containing glass were produced by milled Fe_3O_4 in SiO_2 (Bender Koch & Jiang et al., 1999). This is also consistent with some limited XRD work done in our laboratories (personal communication from Dr. John Robertson)

Sodium silicates, on the other hand, are likely to be much more soluble and if silicate formation was significant, EPA3050B extractions of sodium should be more effective. If, however, the sequestering process was the result of some other process, the EPA3050B results for sodium should be similar to those of the previous elements.

If, as Senna (2001) predicted, two or more than two different metal-oxygen bonds are involved in a reaction resulting in some acid / base reaction then sodium hydroxide will react with quartz to form sodium silicate Na_2SiO_3, $Na_6Si_2O_7$ $Na_2Si_3O_7$ or similar structure which would be somewhat water soluble, so, naturally will be easily react with acid and should be recoverable by EPA3050B digestion.

As a result of the above, it was decided to try milling sodium hydroxide with quartz. The resulting sodium silicate should be readily soluble and the apparent "loss" would not be observed.

In this experiment, 1%* (0.5 grams NaOH in 49.5 grams silica) NaOH was used milled with silica in a steel milling jar. Two gram samples were taken after 5 minutes, 1 hours, 2 hours, 3 hours, 5 hours, 9 hours, 12 hours, 16 hours, 20 hours and 30 hours respectively. After milling, 1 gram of milled powder from each sample was digested using the EPA3050B method. The result is calculated in ppm which is detected Na vs. total reactant (sodium hydroxide with silica).

* NaOH always contains a certain level of water. The background test recovered only 75% of Na from NaOH, therefore, in fact, there was only a 0.75% of NaOH has input.

The results are shown in Figure 3.5.

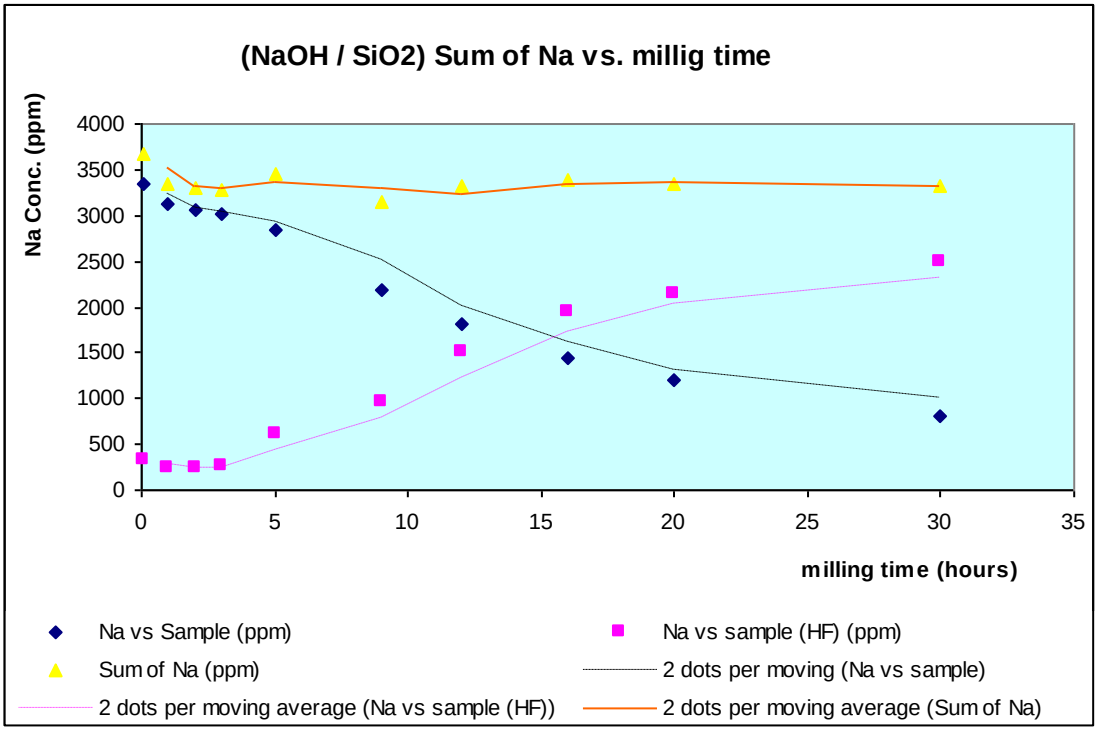

Figure 3.5 The sum of sodium in (NaOH and quartz) milling system, including EPA3050B digestion and HF digestion of the residue.

Summary:

In Figure 3.5 diagram, it can be seen that the NaOH and quartz EPA3050B digestion curve has dropped and is very similar in form to the curves for all the other elements tested previously. As previously, the total recovery (even allowing for the 75% purity of the NaOH) is less than 100%.

The sum of sodium concentration tended to be constant, except for a small valley in the first and second hour samples and it sat at about 3500 ppm level, compared with about 4400 ppm sodium (0.75% NaO and quartz) input. About 75% was recovered.

Comment:

This experiment further confirmed that metals are sequestered by high energy ball milling and cannot be recovered by the EPA3050B method.

These results seem to confirm that the milled final product is not a simple silicate but the metals are being sequestered in a very un-reactive metal-quartz structure.

The unaccounted low recovery of sodium (nearly 25%) is higher than any of the other elements so far tested. It is suspected that it reacted with the milling jar and milling balls (the jars are considered sealed systems and loss as a volatile substance is almost impossible). The observed valley appearing in the first and second hours indicated that the reaction between sodium and the milling jar and balls may be generated in the first hour or even sooner.

3.6 A comparison of the different metals

Since a 5 minutes time interval is used to ensure blending of the system, the detected metal concentration in this sampling time is close to the sum of recovered among (and it can be seen from the above Figures 3.1-2, 3.1-3, 3.2, 3.3-1, 3.4-1 and 3.5, that the detected 5 minutes sample concentration is very close to the sum of detected metal concentration).

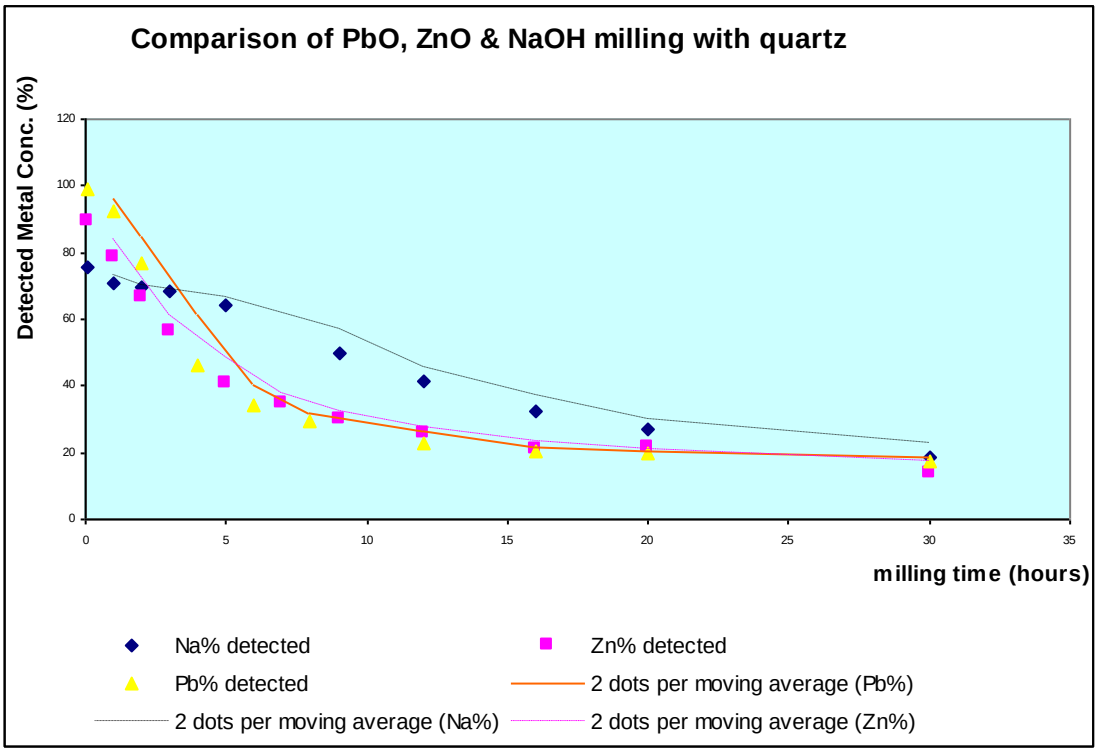

Figure 3.6 Comparison of detected lead, sodium and zinc Conc. (from 0-30 hours); by EPA3050B digestion. (calculated in percentage)

Summary:

It can be seen from this diagram that in the 5 minute sample, almost all the lead has been detected, about 90% of zinc and copper and only about 75% of sodium has been

detected. But in the first 8 hours of milling, the lead concentration dropped most significantly, while the sodium concentration dropped the least significantly and zinc, sat between these values. Lead and zinc reaction slowdown at around 8 hour milling point. But it seems insignificant for sodium on the scale of this diagram. But all of these three elements (lead, zinc, and sodium) reached an average of roughly 15% after 30 hours milling (17% Pb, 14% Zn and 18% Na).

Comment:
It is suspected that during the initial milling period, sodium reacted with the milling balls and jar hence there was only about 75% of the sodium detected at the 5 minute sample but little of the lead had reacted with the balls and jar during that time. This difference may be related to the position of the metal elements in the periodic table, but the mechanism is uncertain.

The slope of the lead line dropped most during the initial 4 hours of milling. Lead is the most "reactive" element when milled with quartz, while sodium is the least reactive.

3.7 Milled particles size distribution

The availability in-house of a laser scattering, particle size analyser provided an interesting addition to the previous work. The change in particle size distribution of the ZnO and quartz samples gave with slightly surprising results.

In the following experiment the particle size of 1% ZnO and quartz milled at 5 minutes, 1 hours, 3 hours, 16 hours, 30 hours, 80 hours and 160 hours have been measured and compared to the raw quartz.

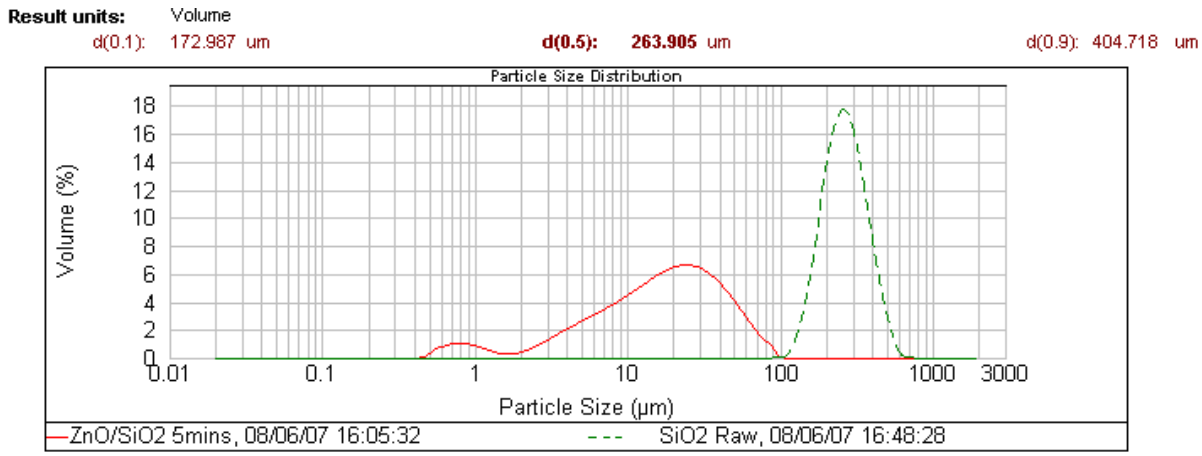

Figure 3.7-1 milled particle size change 0-5 mins

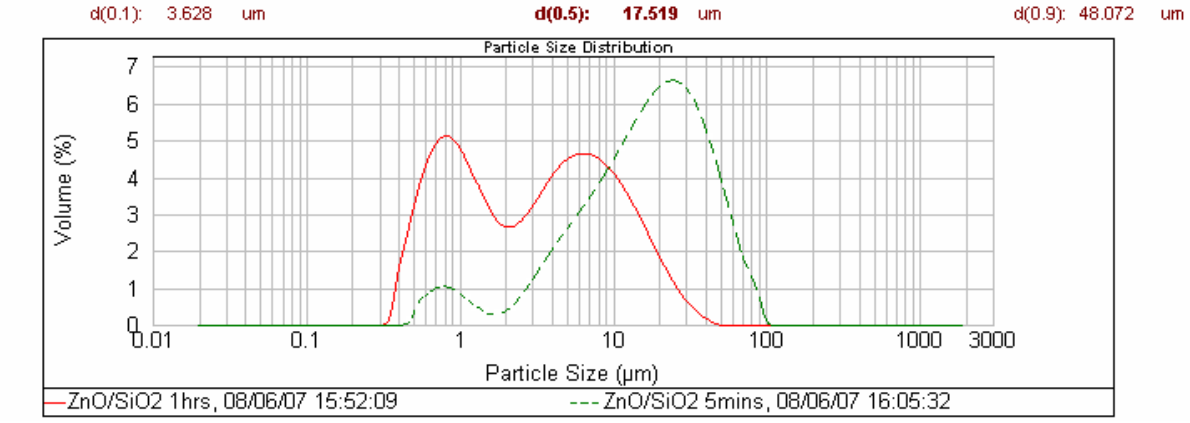

Figure 3.7-2 milled particle size change 5 mins – 1 hour

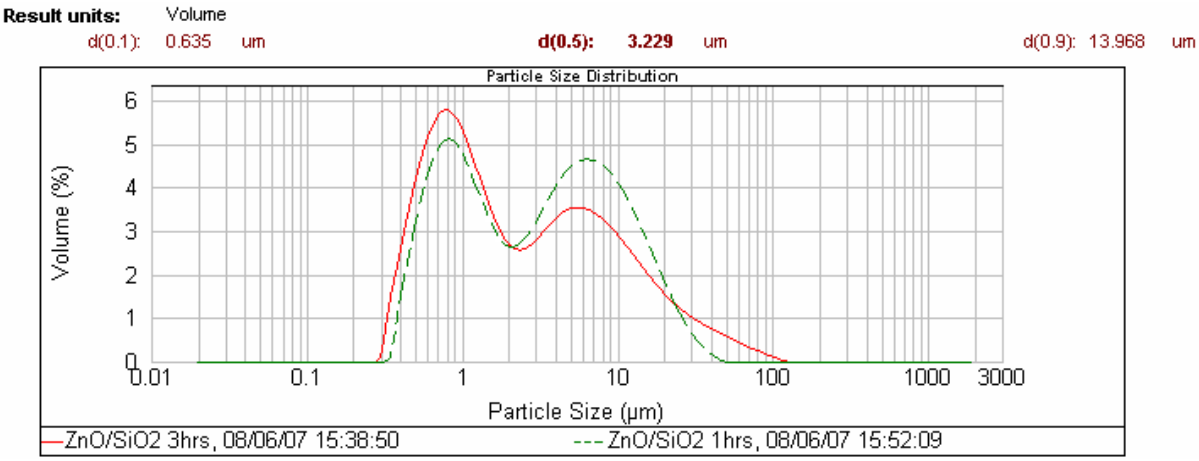

Figure 3.7-3 milled particle size change 1-3 hours

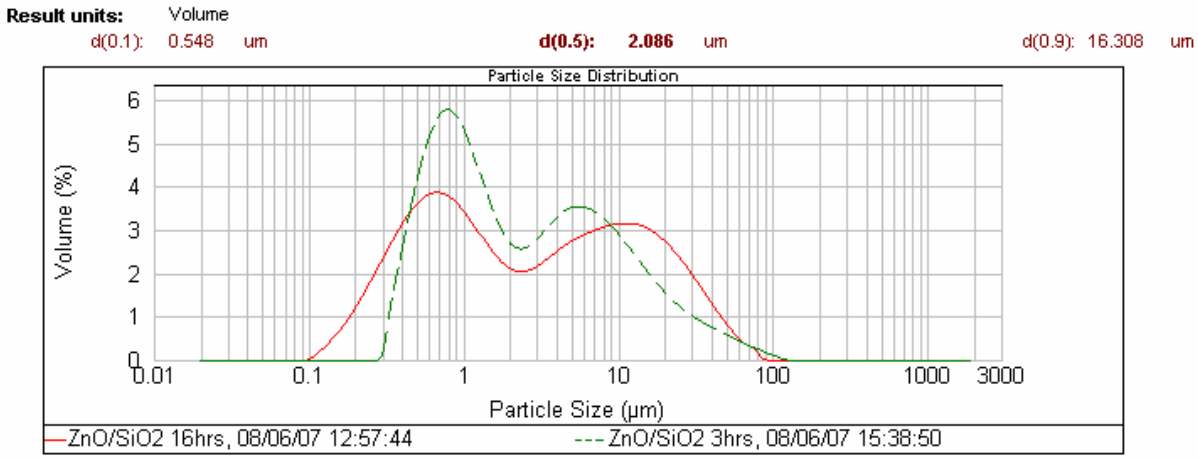

Figure 3.7-4 milled particle size change 3-16 hours

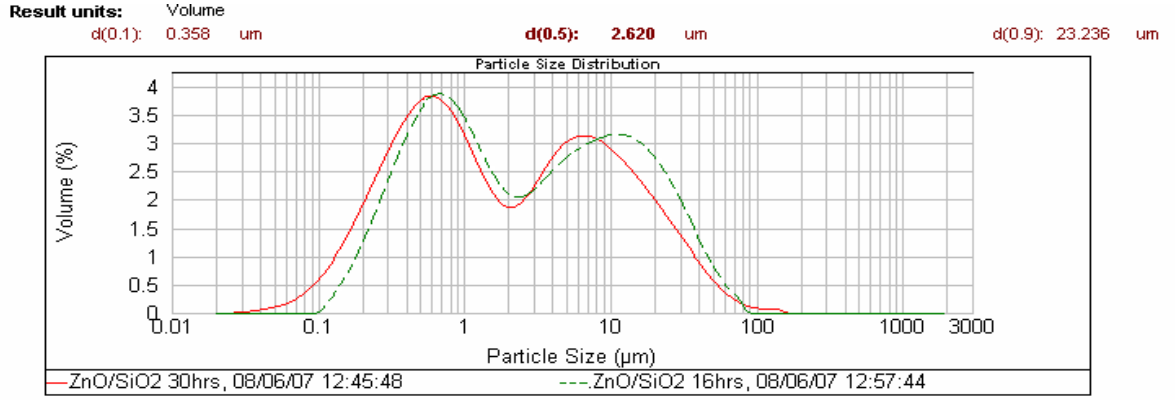

Figure 3.7-5 milled particle size change 16-30 hours

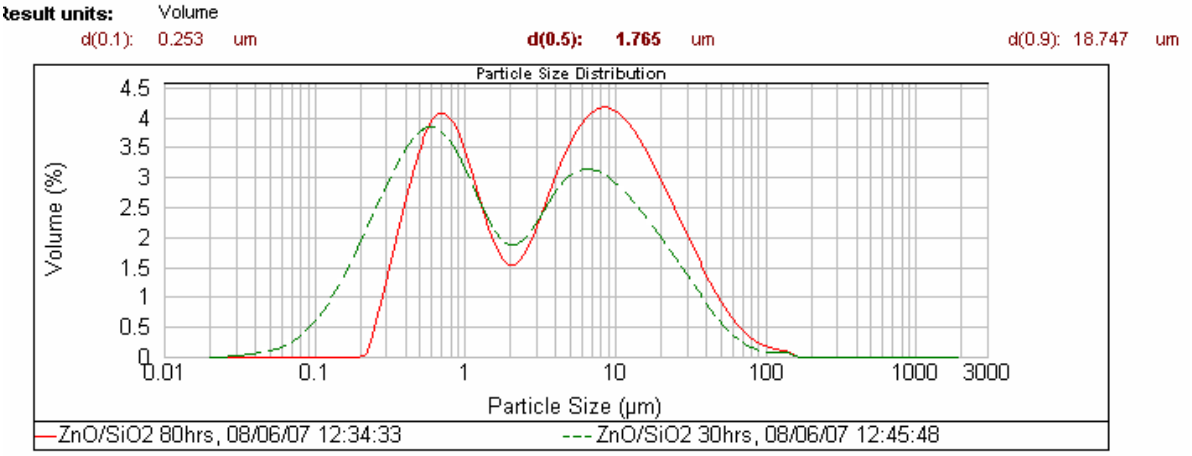

Figure 3.7-6 milled particle size change 30-80 hours

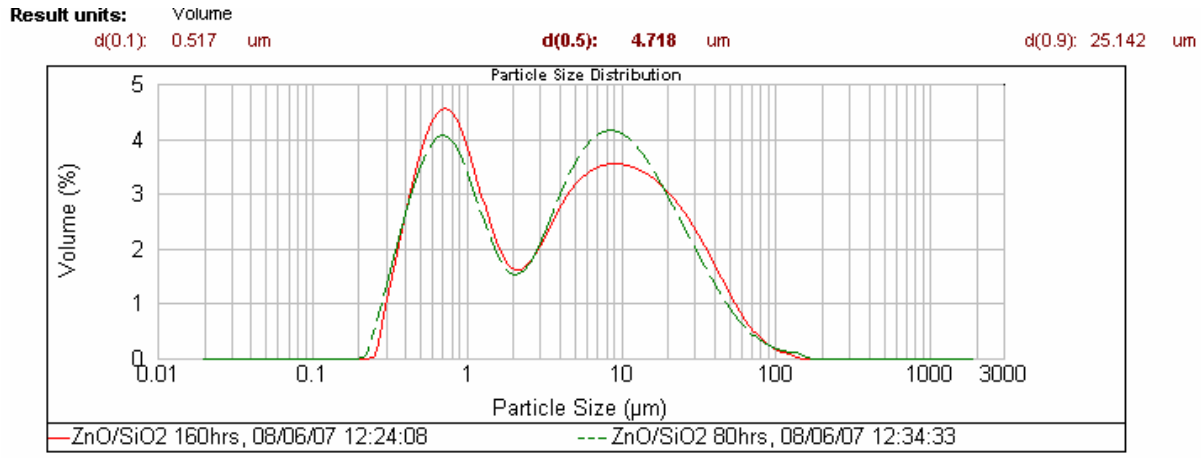

Figure 3.7-7 milled particle size change 80-160 hours

Summary:

Comparing the particle size of raw quartz at 5 minutes milled, 1 hour milled and 3 hours milled quartz, (Figure 3.7-1, Figure 3.7-2 and Figure 3.7-3) it can be seen that in general, the peak of particle size shifted from right (big size) to left (small size) during the initial 3 hours of milling.

There are 2 roughly similar peak heights in the sample milled for 1 hour while the left peak (smaller particle size) is higher than the right peak (bigger particle size) in the 3 hour diagram (Figure 3.7-3). Comparing the 3 hours particles sizes with 1 hour, the left peak (small particle size) of 3 hours is higher than for 1 hour, while the right peak (larger particle size) at 3 hours is lower than that for 1 hour, and there is a small tail created on the right side of the milled 3 hours curve.

It can be seen from Figure 3.7-4 that the left peak of 16 hours is lower than the 3 hour peak but wider than at 3 hours, while the right peak of 16 hours has shifted to the right compared with the 3 hour milled sample. The whole of the 16 hour particle diagram is lower but wider than at 3 hours.

In Figure 3.7-5, peaks shifted a little from the right side (big size, 16 hours particle curve) to the left side (small size, 30 hours particle curve). However, in contrast, peaks shifted from the left side (small size, 30 hours particle curve) to the right side (big size, 80 hours particle curve) in Figure 3.7-6. This time instead of a width reduction in the left peak (small sized peak), the height and width of the right peak (big sized peak)

of 80 hours particle curve greatly increased. These peaks (particle size) remained roughly unchanged up till 160 hours (Figure 3.7-6).

Comment:
In the initial 3 hours milling, the peak of particle size shifted from right to left and instead of a reduction in the right peak, the left peak increased, indicating that, as expected, the quartz particles were being significantly reduced in size. The small tail created on the right side of the 3 hours curve compared with the 1 hour curve indicated that during that period not only were particles broken, but particle synthesis existed as well.

The bimodal nature of the curves suggests that while smaller particles are being formed there are always larger particles present.

Peaks shifted from the left side (30 hours) to the right side (80 hours), indicating that during this period, a significant proportion of particles sintered together. The almost unchanging profile of the 80-160 hours particles size diagram indicated it had reached an equilibrium condition of quartz particle break down and synthesis. (see section 3.8 for the 160 hour milled particle SEM photo).

All these diagrams agree with fragmentation and coalescence events introduced by ball milling (Figure1.3) (Murty & Ranganathan, 1998) which has been discussed in section 1.2.4. Meantime, the particle size change agrees with the three stages proposed by Boldyrev and Avvakumov (1971) in support of the 5 stages (figure 1.4) of mechanochemical synthesis discussed in section 1.2.4.1 and section 1.2.4.4.

The particle size significantly reduces during the first 3 hours of milling, supporting particle size reduction and sharp changes in particle size, causing those small peaks appearing in Figure 3.3-2, 3.3-3, 3.4-3, 3.4-4.

3.8 Scanning Electron Microscopy (SEM) analysis

The literature suggested that, with time some of the milled particles would agglomerate into larger particles (section 1.2.4.4). This was also supported by the particle size measurements (section 3.7).

In order to examine the microstructure of extensively milled quartz, two samples were milled for 160 hours, one with the mild steel balls and the other using the chrome steel balls supplied with the mill. It was expected that the chrome steel balls would exhibit less wear and this may have an effect on the agglomeration of the quartz. The powders formed were analysed by scanning electron microscopy (SEM).

The original sand particles are river worn quartz crystals. After 160 hours milling the resultant particles showed a range of sizes. Although an SEM image is not very representative of a sample, it can be clearly seen that, although there are many particles of 1 µm or less there are also a considerable number in the 10 – 20µm size range. An example of the sample milled with the chrome steel balls is shown in Figure 3.8-1

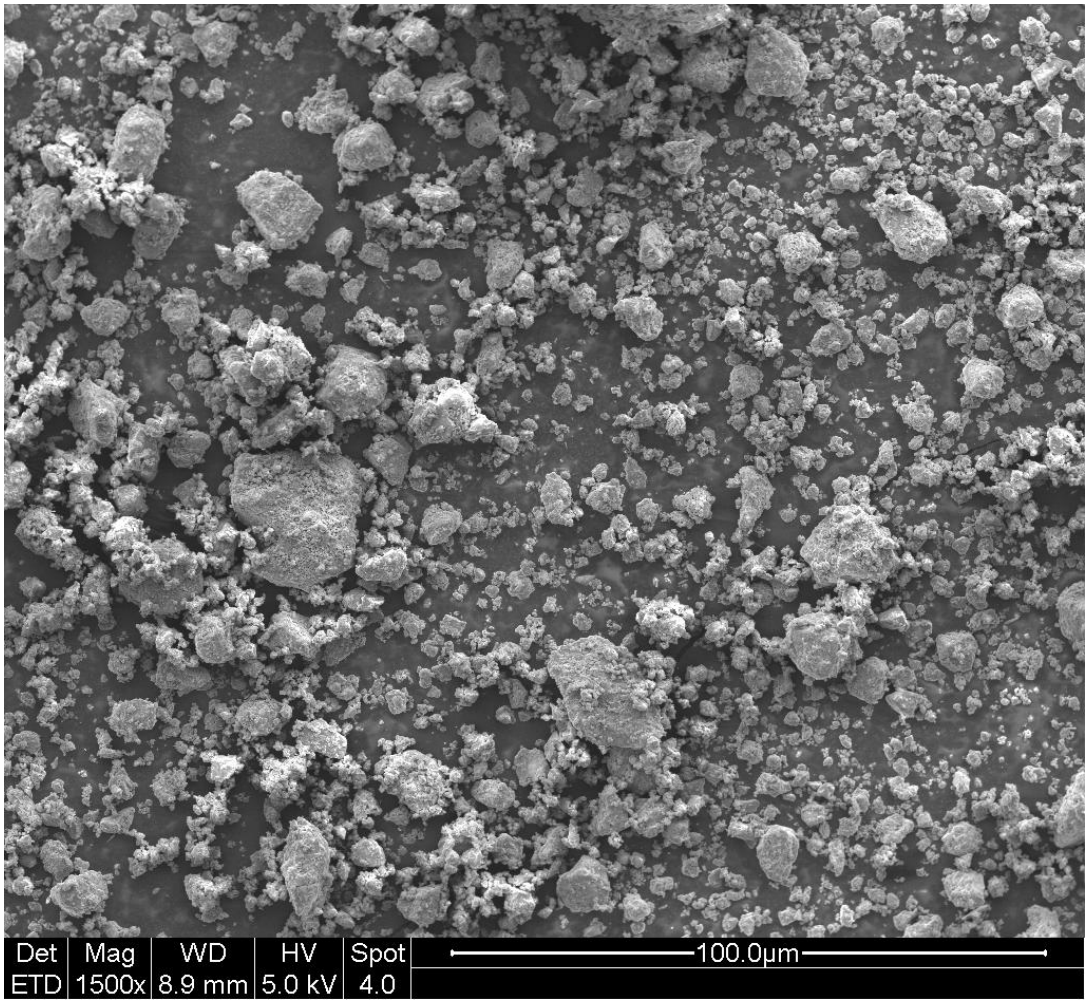

Figure 3.8-1 ZnO and quartz milled 160 hours in chromium jar and balls (100 µm scale)

A closer view of some of the larger particles shows a very clearly agglomerated structure:

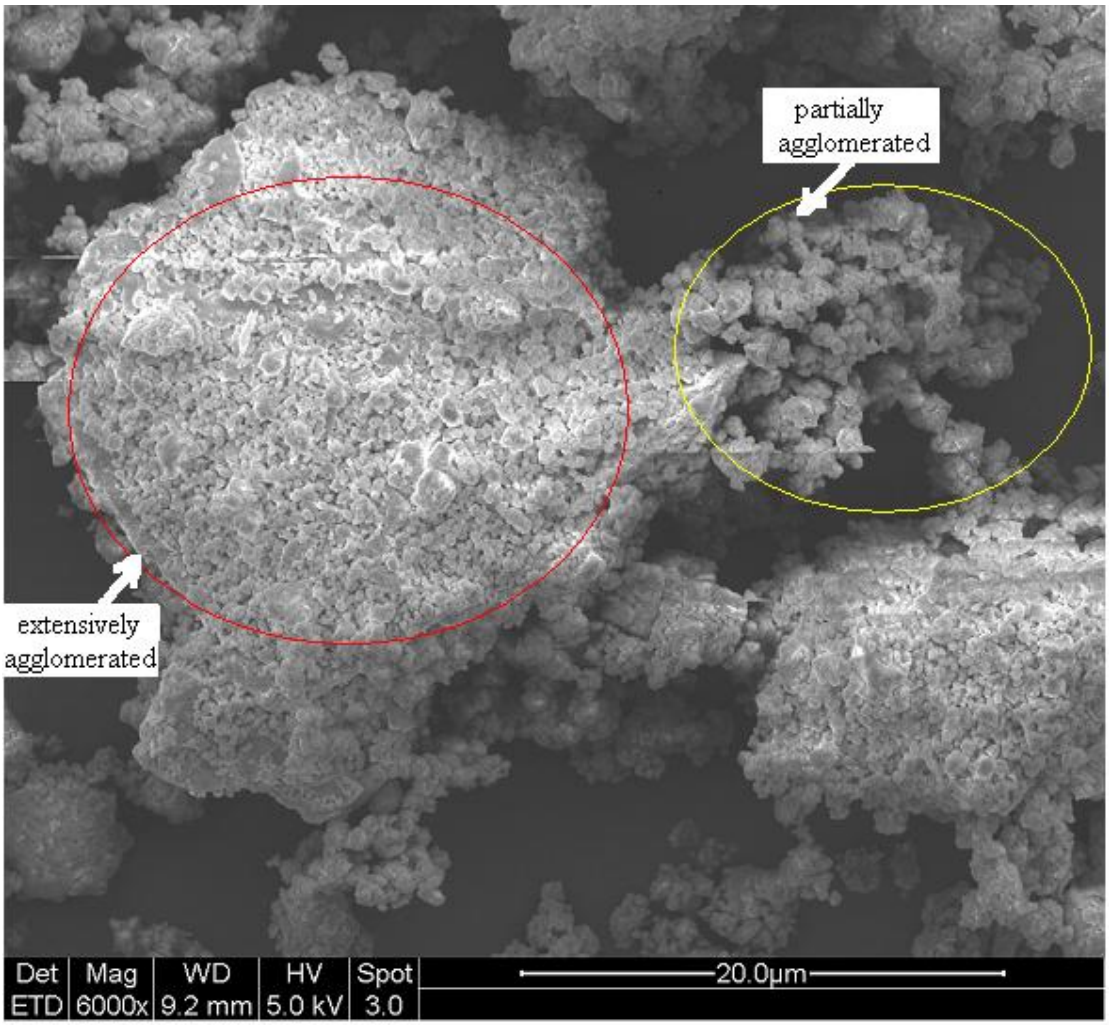

Figure 3.8-2 ZnO and quartz milled 160 hours in chromium jar and balls (20 µm scale)

It can be seen from the above illustration that the central particle is about 20 µm sized and seems to be an extensive agglomeration of small particles, roughly 1 µm in size. To the right of this is a portion showing only partial agglomeration. This may be small particles becoming a lager particle or the larger particle breaking down.

The SEM photo provides evidence of the quartz particle plastic-deformation behaviour which has been discussed in section 1.2.4.4 and this also provided the evidence of the explanation of the particle size changes in section 3.7.

The EDS spectrum is shown below in figure 3.8-3.

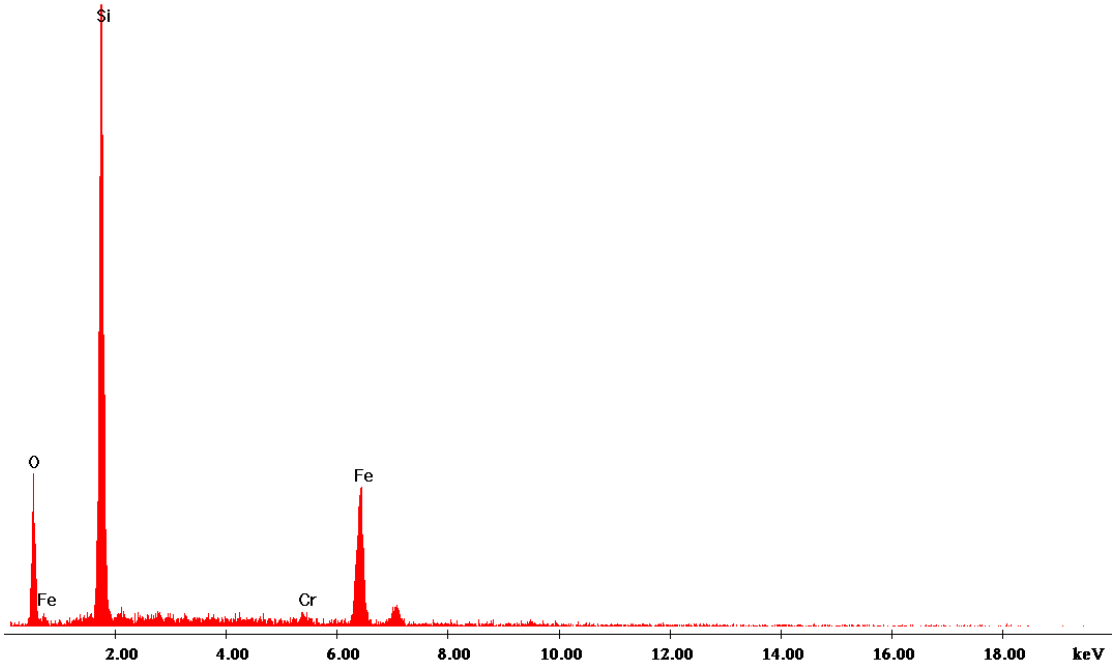

Figure 3.8-3 elements detected by EDS

Without careful comparison to suitable standards, the EDS technique is not very quantitative but if it is assumed that the principle peaks for iron and silicon are approximately proportional to the relative amounts of the two elements, the sample is roughly 20% iron.

This SEM work was not done until the end of the study but an obvious next step will be to compare the amount of EPA extractable iron with the degree of agglomeration.

Chapter 4. Conclusions

This research has provided an answer to the curious "loss" of chloride that Bellingham found in his DDT work (Bellingham, 2006). This work has shown that metal oxides and hydroxides (CuO, MgO, PbO, ZnO and NaOH) could be sequestered with quartz to form structures that bind the metals even in the presence of boiling aqueous acids. Only complete dissolution of the quartz matrix with hydrofluoric acid allowed recovery of the metals.

Although the milling mixture is quite aggressive and wears a considerable amount of iron and chromium from the milling jars, the similarity of results when copper oxide was milled using the zirconia jar and balls or chrome steel jar and balls shows that metallic iron and chromium are not directly involved in the sequestering behaviour. It was also found that changing some other milling conditions, such as ball mass and matrix ratios, had no apparent effect on the sequestering. This strongly suggests that the sequestering process is an intrinsic part of milling with quartz and the trapping seems to be an integral part of the brittle alloying process described earlier in this work.

A very important part of this work has been the analytical methodology. The EPA3050B method is the accepted standard method of quantifying heavy metals in soils. This project has shown that it is not applicable to the analysis of, at least quartz rich matrices after ball milling. An aggressive complete HF based digestion method must be used or results may be low by up to 80%. It can be argued that if the elements are not extractable by the EPA3050B method then they are environmentally unavailable but the EPA3050B method can not be used to answer the question of how much is really there.

This research provided further evidence that the mechanochemical technology could be used as a cost effective way of dealing with industrial wastes. While mechanochemical milling has been shown to effectively destroy organic material (Rowlands & Hall et al., 1994; Bellingham, 2006; Li, 2006), the sequestering that

occurs also has considerable parallel potential as a way of trapping heavy metal pollutants in an insoluble form.

It is highly likely that the sequestering process observed in this work will be found in varying degrees whenever metallic substances are milled with quartz and very likely occurs in various degrees when other brittle minerals are used as the matrix. This has a number of major implications. The first is that analysis of milling products must take account of this if the results are to be used for environmental impact assessment. The second is that it is also probably an integral part of the destruction process for organic material in the milling. The third is that it has the potential to "lock up" environmentally hazardous elements in a simple, environmentally useful way.

Chapter 5. Recommendations for future work

1. For environmental purposes, other matrices, e.g. common minerals like feldspars and other commonly available rocks should be tried.
2. The actual structure of the milled quartz and detail on exactly how the elements are trapped needs to be investigated in more detail.
3. Different milling condition need to be investigated in order to discover how milling parameters affect final product.
4. More elements, (especially non-metals), other salts and compounds should be tried. Ecotoxic elements such as arsenic should probably take some priority.
5. Methods other than the EPA3050B acid extraction and/or other than HF digestion need to be investigated.
6. Lower levels of heavy metals (to simulate the levels commonly found in polluted soils) should be tried.
7. The effect of different milling jars and different mills should be investigated. For example how does a low cost mild steel jar and balls compare to a higher cost chrome steel set.
8. Because living organisms can interact with inorganic materials and solubilise elements from inorganic matrices, extensive biological and microbiological testing would need to be done before the milling process could be used as a way of sequestering environmentally hazardous materials for disposal.
9. Complex oxides with more than three cationic species could be synthesized via a soft-mechanochemical route (Senna, 2001). While there was no direct evidence for this happening in this work this does need further investigation. It may be a way of preparing novel inorganic compounds.

References

Abrahim, G. and R. Parker (2002). "Heavy-metal contaminants in Tamaki Estuary: impact of city development and growth, Auckland, New Zealand." *Environmental Geology* ***42****(8)*: 883-890.

Andrew D. Eaton, Lenore S. Clesceri, et al. (1995). *"Standard Methods for the Examination of Water and Wastewater.*" (ISBN 0-87553-223-3).

Bellingham, T. A. (2006). *"The mechanochemical remediation of persistent organic pollutants and other organic compounds in contaminated soils "* AUT PHD thesis.

Bender Koch, C., J. Z. Jiang, et al. (1999). "Mechanical milling of Fe3O4/SiO2: Formation of an amorphous Fe(II)-Si-O-containing phase." *Nanostructured Materials* ***12****(1-4)*: 233-236.

Benjamin, J. S. (1970). "Dispersion strengthened superalloys by mechanical alloying(Superalloys dispersion strengthening and age hardening by mechanical alloying)." *Metallurgical Transactions* **1**: 2943-2951.

Beyer, M. K. and H. Clausen-Schaumann (2005). "Mechanochemistry: the mechanical activation of covalent bonds." *Chem Rev* ***105****(8):* 2921-48.

Boldyrev, V. V. (1995). "Mechanochemistry and sonochemistry." *Ultrasonics Sonochemistry* ***2****(2)*: S143-S145.

Boldyrev, V. V. and E. G. Avvakumov (1971). "Mechanochemistry of Inorganic Solids." *Russian Chemical Reviews* ***40****(10)*: 847-859.

Boldyrev, V. V. and K. Tkácová (2000). "Mechanochemistry of Solids: Past, Present, and Prospects." *Journal of Materials Synthesis and Processing* ***8****(3):* 121-132.

C.Baldini, N. and et.al (1996). "ASTM Designation: C146 – 94a Standard Test Methods for Chemical Analysis of Glass Sand." *Annual book of ASTM Standards - General Products, Chemical Specialties and End Use Products* ***15.02****(ISBN 0-8031-2347-7):* 1-11.

C.baldini, N. and et.al (1996). "ASTM Designation: E663 – 86 Standard practice for Flame Atomic Absorption Analysis (Re-approved 1991)." *Annual book of ASTM Standards - Metals test methods and Analytical Procedures* ***03.06****(ISBN 0-8031-2291-8):* 200 - 206.

Caër, G. L., T. Ziller, et al. (2000). "Mixing of iron with various metals by high-energy ball milling of elemental powder mixtures." *Hyperfine Interactions* ***V130****(1):* 45-70.

Calka, A., J. I. Nikolov, et al. (1993). "In: deBarbadillo JJ, et al., editors." *Mechanical alloying for structural applications. Materials Park, OH: ASM International*: 189-95.

Chen, Y., B. W. Ninham, et al. (1995). "Replacement reaction induced by ball milling of silica in nitrogen." *Scripta Metallurgica et Materialia* ***32****(1):* 19-22.

Chin, Z. H. and T. P. Perng (1996). "Amorphization of Ni-Si-C ternary alloy powder by mechanical alloying." *Materials Science Forum(Switzerland)* ***235****:* 121-126.

Corrias, A., G. Paschina, et al. (1998). "Ni-silica and Cu-silica nanocomposites prepared by ball milling." *Journal of Non-Crystalline Solids* ***232-234****:* 358-363.

Corrias, A., G. Paschina, et al. (1997). "Ni-SiO 2 nanocomposite powders by high energy ball milling." *Materials Science Forum, vols. 235-238:* 199-204.

CRN, C. f. R. N.-. (Retrieved on 2007). "Nanotechnology Basics: For Students and Other Learners." http://www.crnano.org/basics.htm#questions.

D. F. shriver, P. W. a., C.H.Langford (1996). *"Inorganic Chemistry (Second Edition)."* 154-157.

Deely, J. M., J. C. Tunnicliff, et al. (1992). "Heavy metals insurface sediments of Waiwhetu Stream, Lower Hutt, New Zealand." *New Zealand Journal of Marine and FreshwaterResearch* ***26****:* 417-427.

Delogu, F., C. Deidda, et al. (2004). "A quantitative approach to mechanochemical processes." *Journal of Materials Science* ***39****(16):* 5121-5124.

Delogu, F., R. Orru, et al. (2003). "A novel macrokinetic approach for mechanochemical reactions." *Chemical Engineering Science* ***58****(3):* 815-821.

Dickinson, W. W., G. B. Dunbar, et al. (1996). "Heavy metal history from cores in Wellington Harbour, New Zealand." *Environmental Geology* ***27****(1):* 59-69.

Dunlap, R. (2000). "Materials preparation by ball milling." *Canadian Journal of Physics* ***78****(3):* 211-229.

El-Eskandarany, M. S., K. Aoki, et al. (1990). "Rod Milling for Solid-State Formation of Al sub 30 Ta sub 70 Amorphous Alloy Powder." *Journal of the Less-Common Metals* ***167****(1):* 113-118.

Fernández-Bertran, J. F. (1999). "Mechanochemistry: an overview." *Pure Appl Chem* ***71****(4):* 581-586.

Field, L. D., S. Sternhell, et al. (1997). "Mechanochemistry of some hydrocarbons." *Tetrahedron* ***53****(11):* 4051-4062.

Fuentes, A. F., E. Rodríguez-Reyna, et al. (2006). "Room-temperature synthesis of apatite-type lanthanum silicates by mechanically milling constituent oxides." *Solid State Ionics* ***177****(19-25):* 1869-1873.

Gacitua, W., A. Ballerini, et al. (2005). "Polymer Nanocomposites: Synthetic and Natural Fillers a Review." *Maderas, Cienc. tecnol* ***7****(3):* 159-178.

Gerasimov, K. B., A. A. Gusev, et al. (1991). "Tribochemical equilibrium in mechanical alloying of metals." *Journal of Materials Science* ***26****(9):* 2495-2500.

Gilman, J. J. (1996). "Mechanochemistry." Science **274**(5284): 65.

H.R. Li, D. Q. Z., A.P. Qv, D.R. Sha (1994). " Methods of chemical analysis of sodalime-alumina and borosilicateglass, UDC 666.123:543.06 (GB/T 1549-94)." 国家技术督局发布.

Hasegawa. M, A. Y., Kanda.Y (1995). "Mechanochemical Polymerization of Methyl Methacrylate Initiated by the Grinding of Inorganic Compounds." *Journal of Applied Polymer Science* ***55****:* 297-304.

Heinicke, G. (1984). "Tribochemistry, Akad." Verl., Berlin.

Hong, L. B., C. Bansal, et al. (1994). "Steady state grain size and thermal stability of nanophase Ni sub 3 Fe and Fe sub 3 X(X= Si, Zn, Sn) synthesized by ball milling at elevated temperatures." *Nanostructured Mater.* ***4****(8):* 949-956.

Jiang, J. Z., Y. X. Zhou, et al. (1996). "Microstructural evolution during high energy ball milling of Fe2O3-SiO2 powders." *Nanostructured Materials* ***7****(4):* 401-410.

Kis-Varga, M. and D. L. Beke (1995). "Phase transitions in Cu-Sb systems induced by ball milling." *Materials Science Forum(Switzerland)* ***225****(1):* 465-470.

Koch, C. C., O. B. Cavin, et al. (1983). "Preparation of ‘‘amorphous’’NiNb by mechanical alloying." *Applied Physics Letters* ***43****:* 1017.

Kondo, S., M. Kuzuya, et al. (2002). "Development of Polymeric Prodrugs as a Therapeutic Agent for Alzheimer’s Disease by Mechanochemical Solid-State Polymerization." *Current Medicinal Chemistry Central Nervous System Agents* ***2****(2):* 157-173.

Kuhrt, C. (1993). "Magnetic Properties of Nanocrystalline Mechanically Alloyed Fe-M." *IEEE Transactions on magnetics* **29**.

Kwon, Y.-S., K. B. Gerasimov, et al. (2002). "Ball temperatures during mechanical alloying in planetary mills." *Journal of Alloys and Compounds* ***346****(1-2):* 276-281.

Li, Y. Y. (2006). "reactive milling of organic compounds." *AUT master thesis*

Locci, A. M., R. Orru, et al. (2006). "Effect of ball milling on simultaneous spark plasma synthesis and densification of TiC-TiB2 composites." *Materials Science and Engineering: A* ***434****(1-2):* 23-29.

Luche, J. L. (1992). "Developments of the new'experimental theory' of sonochemistry initiated in Grenoble." *Ultrasonics* ***30****(3):* 156-162.

Martin, K. B. and C.-S. Hauke (2005). "Mechanochemistry: The Mechanical Activation of Covalent Bonds." *Chemical Reviews* ***105****(8):* 2921.

Masahiro Hasegawa, Y. Akiho, et al. (1995). "Mechanochemical Polymerization of Methyl Methacrylate Initiated by the Grinding of Inorganic Compounds." *Journal of Applied Polymer Science* ***55****:* 297-304.

McCormick, P. G. and F. H. Froes (1998). "The fundamentals of mechanochemical processing." *JOM* ***50****(11):* 61-65.

McLay, C. L. (1976). "An inventory of the status and origin of New Zealand estuarine systems." *Proceedings of the New Zealand Ecological Society* ***23****:* 8-26.

Millet, P. and T. Hwang (1996). "Fabrication of TiB2 & TiB2/FeB composites by mechanically activated borothermic reduction of ilmenite." *J. Mater. Res* **11**(4).

Murty, B. S. and S. Ranganathan (1998). "Novel materials synthesis by mechanical alloying/milling." *International materials reviews* ***43****(3):* 101-141.

Nguyen, T. Q., Q. Z. Liang, et al. (1997). "Kinetics of ultrasonic and transient elongational flow degradation: a comparative study." *Polymer* ***38****(15):* 3783-3793.

Obrovac, M. N., O. Mao, et al. (1998). "Structure and electrochemistry of LiMO2 (M=Ti, Mn, Fe, Co, Ni) prepared by mechanochemical synthesis." *Solid State Ionics* ***112****(1-2):* 9-19.

Padella, F., E. Paradiso, et al. (1991). "Mechanical Alloying of the Pd--Si System in Controlled Conditions of Energy Transfer." *Journal of the Less-Common Metals(Switzerland)* ***175****(1):* 79-90.

Puclin, T. and W. A. Kaczmarek (1997). "A high temperature X-ray diffraction study of the crystallisation of amorphous ball-milled zircon." *Colloids and Surfaces A: Physicochemical and Engineering Aspects* ***129-130****:* 365-375.

Retsch (2006). (retriveved on 2007) "Retsch Product Navigator." Retsch Users Guide, http://www.retsch.com/dltmp/www/808b12c73a43c42cdfd57224c6296b12/brochure_ball_mills_en.pdf.

Rowlands, S. A., A. K. Hall, et al. (1994). "Destruction of toxic materials." *Nature* ***367****(6460):* 223-223.

Schwarz, R. B. and W. L. Johnson (1983). "Formation of an Amorphous Alloy by Solid-State Reaction of the Pure Polycrystalline Metals." *Physical Review Letters* ***51****(5):* 415-418.

Senna, M. (2001). "Charge transfer and hetero-bonding across the solid–solid interface at room temperature." *Materials Science & Engineering A* ***304****:* 39-44.

Smith, A. P., H. Ade, et al. (2000). "Cryogenic Mechanical alloying of poly (methyl methacrylate) with polyisoprene and poly (ethylene-alt-propylene)." *Macromolecules* ***33****(7):* 2595-2604.

Sohma, J. (1989). "Mechanochemistry of Polymers." *Prog. Polym. Sci.* **14**(4): 451-596.

Stoffers, P., G. P. Glasby, et al. (1986). "Heavy metal pollution in Wellington Harbour." *New Zealand Journal of Marine and Freshwater Research* ***20****(3):* 495-512.

Suryanarayana, C. (1992). "Milling maps for phase identification during mechanical alloying." *Scripta Metallurgica et Materialia* ***26****(11):* 1727-1732.

Suryanarayana, C. (2001). "Mechanical alloying and milling." *Progress in Materials Science* ***46****(1):* 184.

Suryanarayana, C., E. Ivanov, et al. (2001). "The science and technology of mechanical alloying." *Materials Science and Engineering* ***304****(306):* 151-158.

Takacs, L. and J. S. McHenry (2006). "Temperature of the milling balls in shaker and planetary mills." *Journal of Materials Science* ***41****(16):* 5246-5249.

Thompson, L. H. and L. K. Doraiswamy (1999). "Sonochemistry: science and engineering." *Ind. Eng. Chem. Res* ***38****(4):* 1215-1249.

Tkacova, K., N. Stevulova, et al. (1995). "Contamination of quartz by iron in energy-intensive grinding in air and liquids of various polarity." *Powder Technology* ***83****(2):* 163-171.

Tzvetkov, G. and N. Minkova (2000). "Mechanochemically induced formation of La2SiO5." *Journal of Materials Science* ***35****(10):* 2435-2441.

US.EPA (2003) (Retrieved on 2007). "EPA 3050B: Acid Digestion of Sediments, Sludges and Soils." http://www.epa.gov/SW-846/pdfs/3050b.pdf.

Walch, S. P. and R. C. Merkle (1998). "Theoretical studies of diamond mechanosynthesis reactions." *Nanotechnology* ***9****(3):* 285-296.

Wikipedia (2007). (Retrieved on 2007) "Heavy metals." http://en.wikipedia.org/wiki/Heavy_metals.

Xi, S., J. Zhou, et al. (1996). "The reduction of CuO by Si during ball milling." *Journal of Materials Science Letters(UK)* ***15****(7):* 634-635.

Yamada, K. and C. C. Koch (1993). "The influence of mill energy and temperature on the structure of the TiNi intermetallic after mechanical attrition." Journal of *Materials Research* ***8****(6):* 1317-1326.

Zhao, L., J. Zwick, et al. (2003). "The influence of milling parameters on the properties of the milled powders and the resultant coatings." *Surface and Coatings Technology* ***168****(2-3):* 179-185.

Zhu, M., X. Z. Che, et al. (1998). "Mechanical alloying of immiscible Pb-Al binary system by high energy ball milling." *Journal of Materials Science* ***33****(24):* 5873-5881.

Appendix

Appendix – 1 ICP operation parameters

. Method Report 1/10/2007, 16:15:20

Method Parameters

Analysis Lines

Label	El	Wavelen.	Type	I/S	Bkg Mode	OBCL	OBCR	Peak Track(nm)	Grating Order
Na 330.237	Na	330.237	Analyte	-	Poly			0.0800	1

Conditions Sets (All lines share a single condition set)

Pwr(kW)	PlasFlow(L/min)	AuxFlow(L/min)	NebPres(kPa)	Replicate Time(s)	Stab Time(s)
1.20	15.0	1.50	200.00	1.000	15

PMT Voltage(V)
650

Sample Introduction

Sample Uptake(s)	Rinse Time(s)	Pump Rate(rpm)	Fast Pump
30	10	15	On

General Settings

Replicates	Scan Window (1st order nm)
3	0.120

Calibration Settings

Calib. Mode	No. Standards	Corr Coeff Limit	Reslopes
Quantitative	4	0.995000	Off

Standard Concentration

El	Units	Standard 1	Standard 2	Standard 3	Standard 4
Na	mg/L	1.00000	10.00000	50.00000	100.00000

Calibration Parameters

Label	Thru. Blk	W/Fit	Curve Type	Max Error	Min Conc	Max Conc	E/Curve %	U/Curve %
Na 330.237	On	Off	Linear	50.0	0.00000	110.00000	25	400

Units

Unit Name	Multiplier	Divider
mg/L	1	1E6

Columns

Column
Na 330.237

Display Column Flags

Column	o	QC	S	e	c	i	n	a	u	v	x	b	p	m	d
Na 330.237	x	x	x	x	x	x	x	x	x	x	x	x	x		

. Method Report 14/05/2007, 17:11:30

Method Parameters

Analysis Lines

Label	El	Wavelen.	Type	I/S	Bkg Mode	OBCL	OBCR	Peak Track(nm)	Grating Order
Cr 267.716	Cr	267.716	Analyte	-	Poly			0.0400	2
Cu 324.754	Cu	324.754	Analyte	-	Poly			0.0400	2
Fe 259.940	Fe	259.940	Analyte	-	Poly			0.0400	2
Mg 279.079	Mg	279.079	Analyte	-	Poly			0.0400	2
Pb 220.353	Pb	220.353	Analyte	-	Poly			0.0270	3
Zn 472.216	Zn	472.216	Analyte	-	Poly			0.0800	1

Conditions Sets (All lines share a single condition set)

Pwr(kW)	PlasFlow(L/min)	AuxFlow(L/min)	NebPres(kPa)	Replicate Time(s)	Stab Time(s)
1.20	15.0	1.50	200.00	1.000	15

PMT Voltage(V)
650

Sample Introduction

Sample Uptake(s)	Rinse Time(s)	Pump Rate(rpm)	Fast Pump
30	10	15	On

General Settings

Replicates	Scan Window (1st order nm)
3	0.120

Calibration Settings

Calib. Mode	No. Standards	Corr Coeff Limit	Reslopes
Quantitative	4	0.995000	Off

Standard Concentration

El	Units	Standard 1	Standard 2	Standard 3	Standard 4
Cr	mg/L	1.00000	10.00000	50.00000	100.00000
Cu	mg/L	1.00000	10.00000	50.00000	100.00000
Fe	mg/L	1.00000	10.00000	50.00000	100.00000
Mg	mg/L	1.00000	10.00000	50.00000	100.00000
Pb	mg/L	1.00000	10.00000	50.00000	100.00000
Zn	mg/L	1.00000	10.00000	50.00000	100.00000

Calibration Parameters

Label	Thru. Blk	W/Fit	Curve Type	Max Error	Min Conc	Max Conc	E/Curve %	U/Curve %
Cr 267.716	On	Off	Linear	20.0	0.00000	110.00000	25	400
Cu 324.754	On	Off	Linear	20.0	0.00000	110.00000	25	400
Fe 259.940	On	Off	Linear	50.0	0.00000	110.00000	25	400
Mg 279.079	On	Off	Linear	20.0	0.00000	110.00000	25	400
Pb 220.353	On	Off	Linear	20.0	0.00000	110.00000	25	400
Zn 472.216	On	Off	Linear	20.0	0.00000	110.00000	25	400

Units

Unit Name	Multiplier	Divider
mg/L	1	1E6

Columns

Column
Cr 267.716
Cu 324.754

Column
Fe 259.940
Mg 279.079
Pb 220.353
Zn 472.216

Display Column Flags

Column	o	QC	S	e	c	i	n	a	u	v	x	b	p	m	d
Cr 267.716	x	x	x	x	x	x	x	x	x	x	x	x	x		
Cu 324.754	x	x	x	x	x	x	x	x	x	x	x	x	x		
Fe 259.940	x	x	x	x	x	x	x	x	x	x	x	x	x		
Mg 279.079	x	x	x	x	x	x	x	x	x	x	x	x	x		
Pb 220.353	x	x	x	x	x	x	x	x	x	x	x	x	x		
Zn 472.216	x	x	x	x	x	x	x	x	x	x	x	x	x		

Appendix – 2 Atomic absorption and emission parameter

Element	Cr	Cu	Fe	Mg	Na	Pb	Zn
Lamp serial	/	2815E	43130	2091V	/	/	1523D
Wavelength (nm)	/	327.6	248.3	202.8	589.0	/	213.9
Slit	/	0.7, high	0.2, high	0.7, high	0.2, high	/	0.7, high
Current (mA)	/	6.0	8.0	6.0	10.0	/	8.0
Integration time	3 (seconds)						
Reading delay	5 (seconds)						
Calibration type	Nonlinear						

Appendix – 3 Metals contain in milling balls

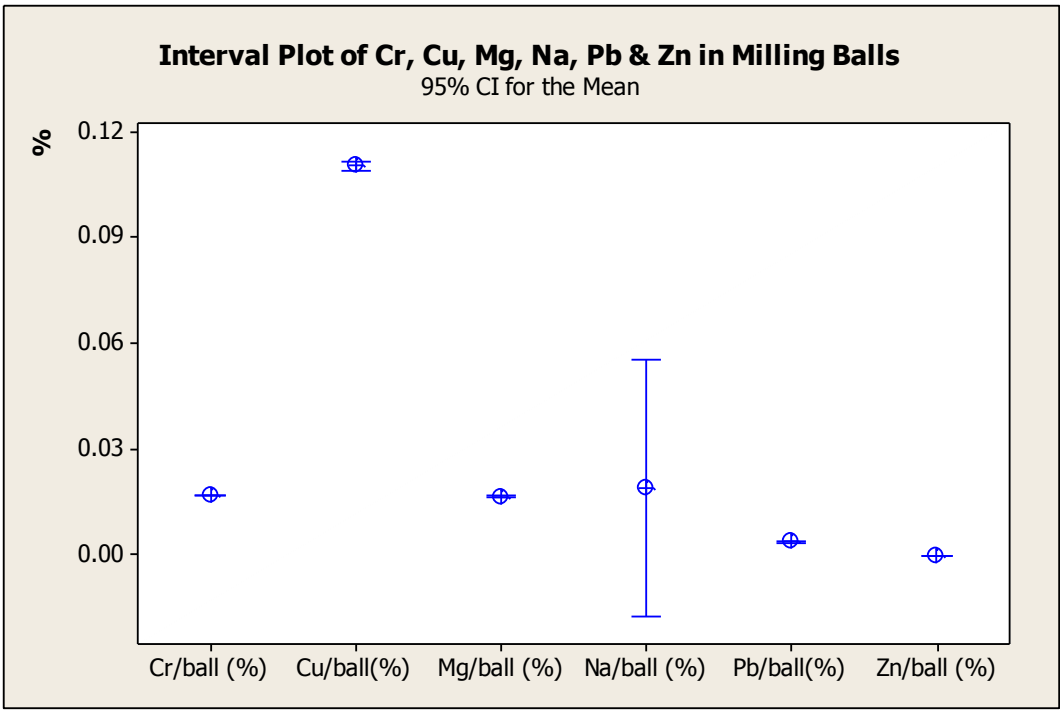

The 95% confidence interval of detected trace metal elements in unmilled quartz and milled quartz by EPA 3050B and HF digestion:

Appendix – 4 Metals contain in milling jar

Materials and Material Analyses
Werkstoffe und Werkstoffanalysen

Retsch®

PM 100/200/400

Grinding jar of stainless steel

Mahlbecher aus rostfreiem Stahl

Material No.: / Werkstoff Nr. :	1.4034	Designation : / Kurzbezeichnung :	X 40 Cr 13
Hardness / Härte	48-52 HRC		
Specific gravity / Dichte	7,8 g/cm³		
Analysis / Analyse	C	00,500 %	
	Fe	82,925 %	
	Cr	14,500 %	
	Si	01,000 %	
	Mn	01,000 %	
	P	00,045 %	
	S	00,030 %	

Grinding jar of chrome steel

Mahlbecher aus Spezialstahl

Material No.: / Werkstoff Nr. :	1.2080	Designation : / Kurzbezeichnung :	X 210 Cr 12
Hardness / Härte	62-63 HRC		
Specific gravity / Dichte	7,85 g/cm³		
Analysis / Analyse	Fe	84,890 %	
	Cr	12,000 %	
	C	02,200 %	
	Mn	00,450 %	
	Si	00,400 %	
	P	00,030 %	
	S	00,030 %	

Grinding jar of tungsten carbide

Mahlbecher aus Wolframcarbid

Material No.: / Werkstoff Nr. :	./.	Designation : / Kurzbezeichnung :	WC
Hardness / Härte	1180-1280 HV 30		
Specific gravity / Dichte	14,8 g/cm³		
Analysis / Analyse	WC	94,000 %	
	Co	6,000 %	

Grinding jar of agate

Mahlbecher aus Achat

Material No.: / Werkstoff Nr. :	./.	Designation : / Kurzbezeichnung :	SiO_2
Hardness / Härte	6,5-7 Mohs		
Specific gravity / Dichte	2,65 g/cm³		
Analysis / Analyse	SiO_2	99,910 %	
	Al_2O_3	0,020 %	
	Na_2O	0,020 %	
	Fe_2O_3	0,010 %	
	K_2O	0,010 %	
	MnO	0,010 %	
	MgO	0,010 %	
	CaO	0,010 %	

Grinding jar of yttrium-partially stabilised zirconium oxide

Mahlbecher aus Yttrium-teilstabilisiertem Zirkonoxid

Material No.: / Werkstoff Nr. :	./.	Designation : / Kurzbezeichnung :	ZrO_2
Hardness / Härte	ca.1200 HV		
	7,5 Mohs		
Specific gravity / Dichte	5,9 g/cm³		
Analysis / Analyse	ZrO_2	94,500 %	
	Y_2O_3	05,200 %	
	SiO_2 / MgO / CaO / Fe_2O_3 / Na_2O / K_2O	<00,300 %	

Index / Inhalt

Appendix – 5 Standard diversion of metals contain in raw quartz

sample	1	2	3	4	5	Std. Dev.
(Unmilled SiO2) Cr vs. SiO2 (ppm)	23.2953	0.5998	5.0929	5.6932	5.1974	8.8082
(Milled SiO2) Cr vs. SiO2 (ppm)	9.3079	4.8995	4.0975	3.6908	5.2915	2.2436
(milled SiO2)HF Cr vs. SiO2(ppm)	18.8633	18.8981	9.4943	5.7357	7.3882	12.0759
(Unmilled SiO2) Cu vs. SiO2 (ppm)	0.8998	2.1993	1.6976	2.7966	1.0995	0.7819
(Milled SiO2) Cu vs. SiO2 (ppm)	5.7431	0.5000	0.8995	-0.0998	0.0000	2.4562
(Milled SiO2)HF Cu vs. SiO2 (ppm)	7.2284	5.3995	5.3968	3.4913	3.4944	1.5673
(Unmilled SiO2) Fe vs. SiO2 (ppm)	100.2799	42.7872	45.4364	65.1219	43.8781	24.5752
(Milled SiO2) Fe vs. SiO2 (ppm)	86.6422	70.6929	82.9502	70.7232	75.6789	7.2238
(Milled SiO2)HF Fe vs. SiO2 (ppm)	185.7115	213.3787	139.9161	153.7157	163.6382	28.8581
(Unmilled SiO2) Mg vs. SiO2 (ppm)	4.8990	5.7983	5.1927	9.2889	4.1979	1.9932
(Milled SiO2) Mg. vs. SiO2	8.6147	5.3992	8.5948	12.1696	10.1837	2.4862
(Milled SiO2)HF Mg vs. SiO2 (ppm)	20.0515	22.2478	17.8893	30.9726	32.0487	6.4680
(Unmilled SiO2) Na vs. SiO2(ppm)	119.0762	156.3531	90.2736	84.2988	132.6337	29.9163
(Milled SiO2) Na. vs. SiO2 (ppm)	164.3836	194.5000	104.5268	106.3362	199.2000	46.1257
(Milled SiO2)HF Na vs. SiO2 (ppm)	91.3952	88.2412	100.3898	95.3616	80.3215	7.5645

(Unmilled SiO2) Pb vs. SiO2 (ppm)	3.7992	0.0000	0.0999	3.1962	0.0000	1.9099
(Milled SiO2) Pb vs. SiO2 (ppm)	1.7824	-0.5000	0.0000	-1.0973	-1.3978	1.2540
(Milled SiO2)HF Pb vs. SiO2 (ppm)	0.9902	1.0499	0.8495	2.1945	2.1466	0.6655
(Unmilled SiO2) Zn vs. SiO2(ppm)	64.4871	45.3864	51.1284	45.3456	60.6697	8.8037
(Milled SiO2) Zn vs. SiO2 (ppm)	39.8059	32.6967	51.1693	48.9776	32.5479	8.7871
(Milled SiO2)HF Zn vs. SiO2 (ppm)	17.4770	12.7987	9.1445	4.9377	3.5443	5.7204

* Negative result is considered as system error within tolerance.

Table Average metal concentration in unmilled and 1 hour (zirconia jar) milled silica

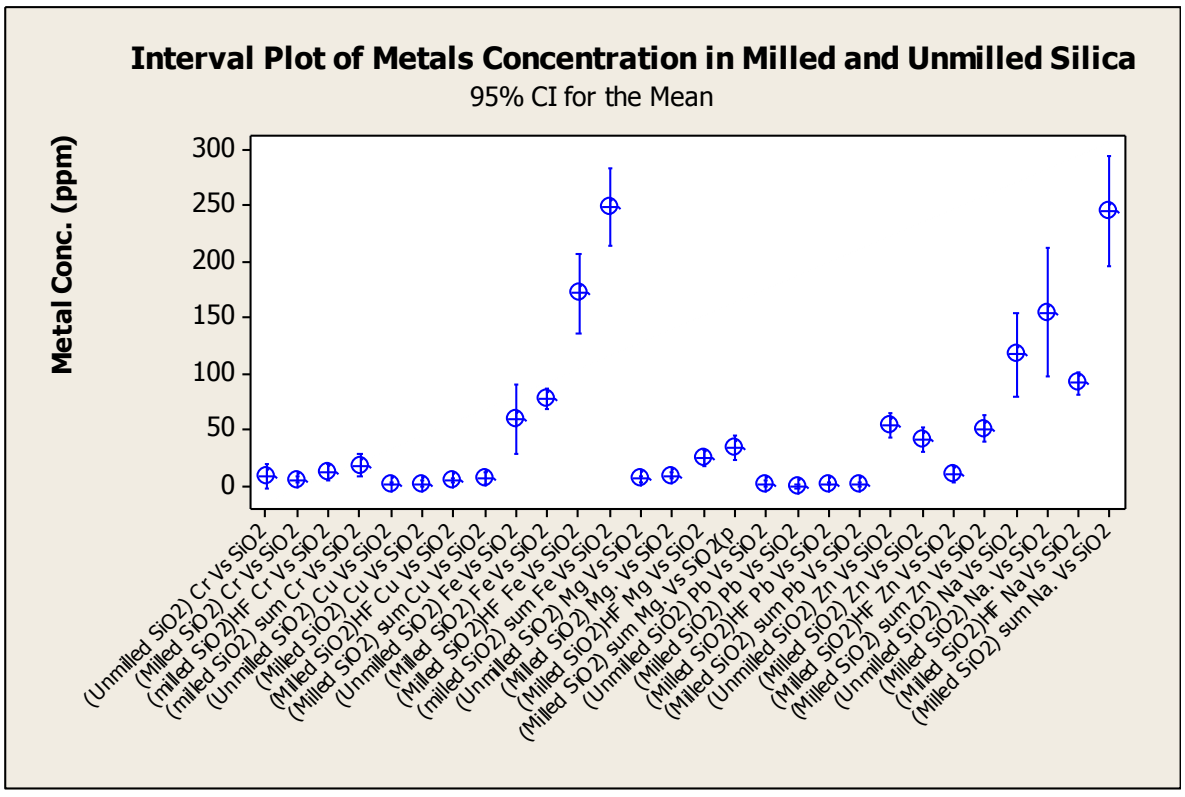

chromium, copper, iron, magnesium, lead, zinc concentration in SiO_2 digested by EPA3050B and HF test (unmilled SiO_2 vs. 1hour milled SiO_2).

Appendix – 6 Quartz background analysis

The difference of metal contain in 1 hour zirconia jar milled quartz and unmilled quartz

---

For the comparison of metals contained in unmilled quartz and milled quartz, Minitab 2-sample T test was used.

Test statistic is P value, if $P < 0.05$ then there is significant difference between the mean concentration of metals contained in the 1 hour zirconia jar milled quartz and in unmilled quartz.

If $P > 0.05$ then there is no significant difference between the metals contained in 1 hour zirconia jar milled quartz and in unmilled quartz.

Two-Sample T-Test and CI: (Unmilled SiO_2) Cr vs. SiO2, (Milled SiO2) Cr vs. SiO2

Two-sample T for (Unmilled SiO2) Cr vs. SiO2 vs. (Milled SiO2) Cr vs. SiO2

	N	Mean	StDev	SE Mean
(Unmilled SiO2)	5	7.98	8.81	3.9
(Milled SiO2) Cr	5	5.46	2.24	1.0

Difference = mu ((Unmilled SiO2) Cr vs. SiO2) - mu ((Milled SiO2) Cr vs. SiO2)
Estimate for difference: 2.51828
95% CI for difference: (-8.76772, 13.80427)
T-Test of difference = 0 (vs. not =): T-Value = 0.62 P-Value = **0.569** DF = 4

Two-Sample T-Test and CI: (Unmilled SiO2) Cu vs. SiO2, (Milled SiO2) Cu vs. SiO2

Two-sample T for (Unmilled SiO2) Cu vs. SiO2 vs. (Milled SiO2) Cu vs. SiO2

	N	Mean	StDev	SE Mean
(Unmilled SiO2)	5	1.739	0.782	0.35
(Milled SiO2) Cu	5	1.41	2.46	1.1

Difference = mu ((Unmilled SiO2) Cu vs. SiO2) - mu ((Milled SiO2) Cu vs. SiO2)
Estimate for difference: 0.330015

95% CI for difference: (-2.870606, 3.530637)
T-Test of difference = 0 (vs. not =): T-Value = 0.29 P-Value = **0.789** DF = 4

Two-Sample T-Test and CI: (Unmilled SiO_2) Fe vs. SiO_2, (Milled SiO_2) Fe vs. SiO_2

Two-sample T for (Unmilled SiO_2) Fe vs. SiO_2 Vs. (Milled SiO_2) Fe vs. SiO_2

	N	Mean	StDev	SE Mean
(Unmilled SiO2)	5	59.5	24.6	11
(Milled SiO2) Fe	5	77.34	7.22	3.2

Difference = mu ((Unmilled SiO_2) Fe vs. SiO_2) - mu ((Milled SiO_2) Fe vs. SiO_2)
Estimate for difference: -17.8368
95% CI for difference: (-49.6419, 13.9683)
T-Test of difference = 0 (vs. not =): T-Value = -1.56 P-Value = **0.194** DF = 4

Two-Sample T-Test and CI: (Unmilled SiO2) Mg vs. SiO2, (Milled SiO2) Mg. vs. SiO2

Two-sample T for (Unmilled SiO2) Mg vs. SiO2 vs. (Milled SiO2) Mg. vs. SiO2

	N	Mean	StDev	SE Mean
(Unmilled SiO2)	5	5.88	1.99	0.89
(Milled SiO2) Mg	5	8.99	2.49	1.1

Difference = mu ((Unmilled SiO2) Mg vs. SiO2) - mu ((Milled SiO2) Mg. vs. SiO2)
Estimate for difference: -3.11705
95% CI for difference: (-6.48681, 0.25272)
T-Test of difference = 0 (vs. not =): T-Value = -2.19 P-Value = **0.065** DF = 7

Two-Sample T-Test and CI: (Unmilled SiO2) Pb vs. SiO2, (Milled SiO2) Pb vs. SiO2

Two-sample T for (Unmilled SiO2) Pb vs. SiO2 vs. (Milled SiO2) Pb vs. SiO2

	N	Mean	StDev	SE Mean
(Unmilled SiO2)	5	1.42	1.91	0.85
(Milled SiO2) Pb	5	-0.24	1.25	0.56

Difference = mu ((Unmilled SiO2) Pb vs. SiO2) - mu ((Milled SiO2) Pb vs. SiO2)
Estimate for difference: 1.66158

95% CI for difference: (-0.83868, 4.16183)
T-Test of difference = 0 (vs. not =): T-Value = 1.63 P-Value = **0.155** DF = 6

Two-Sample T-Test and CI: (Unmilled SiO2) Zn vs. SiO2, (Milled SiO2) Zn vs. SiO2

Two-sample T for (Unmilled SiO2) Zn vs. SiO2 vs. (Milled SiO2) Zn vs. SiO2

	N	Mean	StDev	SE Mean
(Unmilled SiO2)	5	53.40	8.80	3.9
(Milled SiO2) Zn	5	41.04	8.79	3.9

Difference = mu ((Unmilled SiO2) Zn vs. SiO2) - mu ((Milled SiO2) Zn vs. SiO2)
Estimate for difference: 12.3639
95% CI for difference: (-0.7898, 25.5177)
T-Test of difference = 0 (vs. not =): T-Value = 2.22 P-Value = **0.062** DF = 7

Two-Sample T-Test and CI: (Unmilled SiO2) Na vs. SiO2, (Milled SiO2) Na vs. SiO2

Two-sample T for (Unmilled SiO2) Na vs. SiO2 vs. (Milled SiO2) Na. vs. SiO2
(ppm)

	N	Mean	StDev	SE Mean
(Unmilled SiO2)	5	116.5	29.9	13
(Milled SiO2) Na	5	153.8	46.1	21

Difference = mu ((Unmilled SiO2) Na vs. SiO2(ppm)) - mu ((Milled SiO2) Na. vs. SiO2 (ppm))
Estimate for difference: -37.2622
95% CI for difference: (-97.4241, 22.8996)
T-Test of difference = 0 (vs. not =): T-Value = -1.52 P-Value = **0.180** DF = 6

Conclusion:

Since all the P values calculated by 2-sample T test (Minitab) are over 0.05, it can be confirmed that there is no significant difference between the mean concentration of metals contained in the 1 hour zirconia jar milled quartz and in the mean of unmilled quartz.

Appendix – 7 Standard diversion of detected zinc in ZnO and quartz

by EPA3050B digestion

milling time (hour)	Zn Conc. vs. Solid (AA) -1	Zn Conc. vs Solid (ICP) -2	Zn Conc. vs SiO_2 (1st) -1	Zn Conc. vs SiO_2 (1st) -2	Std Dev.
0.0833	7728.1355	6658.1146	7227.4153	6810.8245	479.4177
1.0000	6794.0347	5902.6892	6336.5301	6069.9409	388.9494
2.0000	5957.3621	5236.3691	5359.5243	5220.5108	348.2018
3.0000	5159.3362	4491.9701	4554.2922	4451.3419	332.7719
5.0000	3811.7217	3118.1180	3285.6997	3254.1251	304.9969
7.0000	3338.4397	2720.5575	2831.2183	2815.9898	278.9252
9.0000	2879.9136	2344.0988	2407.3701	2419.9557	246.9602
12.0000	3045.0215	1967.7579	2064.0686	2085.2887	505.5848
16.0000	2098.5384	1670.0650	1700.3142	1732.4234	200.4259
20.0000	2001.7536	1600.1794	1731.7499	1754.4725	167.5672
30.0000	1584.6546	1074.7384	1100.7783	1101.5765	246.4607